



Natural Climate Drivers Dominate in the Current Warming

Antero Ollila

School of Engineering (Emer.)
Aalto University, Espoo, Finland



Klimarealistene
P.O. Box 33,
3901 Porsgrunn
Norway
ISSN: 2703-9072

Correspondence to

aveollila@yahoo.com

Vol. 3.3 (2023)

pp. 290-327

Abstract

Anthropogenic global warming (AGW) is the prevailing theory of the IPCC for global warming. Greenhouse (GH) gases are the major drivers, whereas albedo, aerosols, and clouds have had cooling effects, and natural drivers have an insignificant role (<0.8 %). According to Assessment Report 6 (AR6), these radiative forcings (RF) have been a total of 2.70 Wm^{-2} causing a temperature increase of $1.27 \text{ }^\circ\text{C}$ in 2019. Many research studies are showing significantly lower RF and climate sensitivity values for anthropogenic climate drivers. Research studies offering natural climate drivers as the partial or total solution for global warming have gradually emerged like solar radiation changes, cosmic forces, and multidecadal, century- and millennial-scale oscillations. The cloud effects are still a major concern in General Circulation Models (GCMs). The cloudiness changes have a major role in cosmic effects like magnifying the warming effect of the Total Solar Irradiation (TSI). The 60- and 88-year oscillations are the best-known oscillations, which are commonly known as AMO (Atlantic Multidecadal Oscillation) and the Gleissberg cycle explaining the ups and downs of the global temperature in the 1900s. Mechanisms of long-term climate oscillations are still under debate. There are also essential differences between carbon cycle models and GH effect magnitude specifications. The synthesis of these natural climate drivers together with anthropogenic drivers constitutes an alternative theory called Natural Anthropogenic Global Warming (NAGW), in which natural drivers have a major role in dominating the warming during the current warm period. These results mean that there is no climate crisis and a need for prompt CO_2 reduction programs.

Keywords: *anthropogenic climate drivers; natural climate drivers; climate sensitivity; radiative forcing; positive water feedback; climate oscillations; carbon circulation; SW radiation anomaly*

Submitted 2023-02-09, Accepted 2023-07-31, Updated 2023-12-26,

<https://doi.org/10.53234/scc202304/03>

1. Introduction

The results of the IPCC are prevailing perceptions of global warming or more commonly climate change. According to AR6 (IPCC, 2021), the contribution of the anthropogenic climate drivers is 99.2 % of the global warming from 1750 to 2019. The model-calculated temperature anomaly according to AR6 in 2019 was $1.27 \text{ }^\circ\text{C}$ and the estimate of the global observed temperature anomaly in 2019 was $1.29 \text{ }^\circ\text{C}$ (IPCC, 2021, Fig. 7-51). The main indicator of global warming is the

surface temperature T_s , and according to IPCC, there is practically no error between the observations and the GCMs in 2019. At first sight, it looks like there is a perfect match between the AGW and the observations. A prompt analysis reveals contradictions.

There is a significant improvement in the model calculated T_s values if compared to the same figures reported in AR5 (IPCC, 2013). The total Radiative Forcing (RF) was 2.34 Wm^{-2} in 2011. Using the Climate Sensitivity Parameter (λ) value of $0.5 \text{ K}/(\text{Wm}^{-2})$, the model calculated temperature T_s increase was $1.17 \text{ }^\circ\text{C}$. This figure is 37.6 % greater than the observed temperature anomaly of $0.85 \text{ }^\circ\text{C}$ in 2011. This temperature anomaly has increased to $1.29 \text{ }^\circ\text{C}$ in 2019. The reasons for this abrupt temperature increase should be identified since GH gases are not able to cause such an increase according to the IPCC.

The testimony of Christy (2017) in the U.S. House Committee on Science 2017 contains the description of the scientific test between the 102 CMIP5 climate model runs (CMIP5 means Coupled Model Intercomparison Project Phase 5 experiment design) and the tropical mid-tropospheric temperature from 1979 to 2016. The observed temperatures consist of satellites, balloons, and model-computed temperatures called reanalyze. In the test was applied the F-Test method of Vogelsang-Franses designed to determine whether the trends of the two time series are equivalent or significantly different. The test values showed that all three observational temperature trends were highly significantly different (99 % confidence level) than the average of 102 CMIP5 models. The error between the average 102 CMIP5 models and the satellite temperature was about $0.55 \text{ }^\circ\text{C}$ during the period from 2010 to 2015.

Together, 16 scientists have published an article (Santer et al., 2017) in which they realize that “*Over most of the early twenty-first century, however, model tropospheric warming is substantially larger than observed; warming rate differences are generally outside the range of trends arising from internal variability.*”

One of the objectives of this paper is to challenge the IPCC’s climate change science. The most important issues of global warming are the RF magnitude of CO_2 , the positive water feedback, transient climate response (TCR), and the relative strengths of greenhouse (GH) gases. The first objective of this review study is to find out and analyze the anthropogenic contributions according to the competing research studies not applied by the IPCC. Since these issues are the most important, the theoretical aspects will be analyzed thoroughly.

The second objective is to analyze the anthropogenic carbon amount in the atmosphere and its residence time, which are the basis for the scenario calculations during this century. The third objective is to analyze the GH effect specification of the IPCC, which is “IPCC-made” and conflicts with the IPCC policy to apply only reviewed research results. There are alternative specifications not considered by the IPCC. The GH effect specification of the IPCC does not affect global warming calculations, but it creates a strong GH gas image for CO_2 .

The contributions of alternative research studies of anthropogenic climate drivers are usually much lower than those of the IPCC. Therefore, natural climate drivers are needed for filling up the gap. The IPCC omits almost totally the long-term solar radiation changes, cosmic forces, and multidecadal, century- and millennial-scale oscillations as drivers of global warming. The fourth objective is to summarize and analyze the differences between AGW and NAGW.

2. Materials and methods

The material and data applied to the IPCC reports and mainly the newest AR6 (IPCC, 2021) constitute the reference basis for analyses. The scientific papers, which may not have been referred to by the IPCC, constitute another source of results and data. The approach of this review study is to analyze critically the results of the IPCC and to compare them to the alternative research papers, which we could call research studies of contrarians. The RF value of CO_2 and the positive water

feedback have decisive roles in the IPCC science and therefore these issues have been analyzed thoroughly.

3. Results

3.1 The strength of carbon dioxide (CO₂) as a GH gas

The RF value calculated at the tropopause was called instantaneous radiative forcing (IRF) in the AR5, and at the top of the atmosphere (TOA), the IPCC (2013) used the term Effective Radiative Forcing (ERF). The IPCC changed the terminology and the specifications of RF terms in the AR6 (IPCC, 2021). The Instantaneous Radiative Forcing (IRF) was defined now as the change in the net TOA (Top of the Atmosphere) radiative flux following a perturbation, excluding any adjustments. The Stratospheric Temperature-adjusted Radiative Forcing (SARF) was defined as the change in the net radiative flux at the TOA following a perturbation, including the response to stratospheric temperature adjustments.

The ERF is the final RF at the TOA for a particular forcing agent, and it is the sum of the IRF and the adjustments. The AR6 refers to four RF studies, which have practically the same ERF results but essential differences in calculation methods. The RF value of CO₂ caused the concentration increase from 280 ppm to 560 ppm has been marked as 2*CO₂ and it is needed in calculating climate sensitivity values as temperature changes. The 2*CO₂ of Myhre et al. (1998) is 3.71 Wm⁻², and it is based on spectral calculations at the tropopause with stratospheric adjustments. This value has been used by the IPCC in three previous Assessment Reports, namely TAR (IPCC, 2001), AR4 (IPCC, 2007), and AR5 (IPCC, 2011). In 2010 Schmidt et al. (2010) called this value a canonical estimate as it seemed to be unchallenged. In AR6 the IPCC writers introduced a higher 2*CO₂ on questionable rationale. In the AR6 three other 2*CO₂ values have been referred namely the 3.75 Wm⁻² of Etminan et al. (2016) and the 3.75 Wm⁻² of Meinshausen et al. (2020) are based on spectral calculations at the TOA by using the Oslo LBL code (Myhre et al., 2016). The 2*CO₂ of Smith et al. (2018) the 3.70 Wm⁻² and is based on the simulation of 11 GCMs applying the average IRF values at the TOA and the adjustments.

Finally, the IPCC (2021) formulated a new presentation not found in these referred scientific papers, since they replaced IRF with SARF. The IPCC formulated a new paradigm, and the ERF of 3.93 Wm⁻² is 5.3 % greater than in the three referred studies above from 3.7 Wm⁻² to 3.75 Wm⁻².

A simple mathematical formula is available for calculating RF values for other concentration values. The original equation of Myhre et al. (1998) for calculating the RF value of CO₂ was

$$RF = k * \ln(C/560) [Wm^{-2}] \quad (1)$$

where $k = 5.35$, and C is the concentration of CO₂ (ppm). It should be noticed that RF is radiative forcing change due to the external climate driver changes, which may have happened since 1750. The values of this equation are a little bit lower than that of the official RF values of AR6 (IPCC, 2021), but the IPCC does not introduce the equation giving a 2*CO₂ value of 3.93 Wm⁻². Eq. (1) gives the RF value of 2.06 Wm⁻² for CO₂ concentration 411.7 ppm in 2019, and the same value in AR6 (IPCC, 2021, Fig. 7.6)) is 2.16 Wm⁻², which is 4.9 % greater being in line with the 2*CO₂ values.

There are different 2*CO₂ values, which are not referred to in the AR6 (IPCC, 2021). Barrett et al. (2006) and Schildknecht (2020) have applied LBL (line-by-line) calculations and their values are

3.1 Wm⁻² and 3.0 Wm⁻². Wijngaarden and Happer (2020) achieved a 2*CO₂ value of 3.0 Wm⁻² based on their LBL calculations using the HITRAN database (2021). Their RF value for 2*CO₂ (from 400 ppm to 800 ppm) of 3.0 Wm⁻² is at the altitude of 86 km, and the same value at 11 km is 5.5 Wm⁻², which has not been explained.

Harde (2013) also applied his own LBL calculations and his two-layer atmospheric model. His 2*CO₂ value is 2.4 Wm⁻². Miskolczi and Mlynczak (2004) carried out extensive LBL calculations with different atmospheric compositions, and their 2*CO₂ value is 2.53 Wm⁻².

Ollila (2014) has reported a 2*CO₂ of 2.16 Wm⁻² utilizing LBL calculations with the Spectral Calculator tool (GATS, 2021) by using the HITRAN (2021) database and water-continuum model. Ollila's calculations are in line with Ohmura (2001) that 98 % of total LW absorption happens in the troposphere, and therefore the CO₂ absorption does not increase in the stratosphere, but it is saturated before the altitude of 1 km. The IRF value (the RF at the troposphere) of Smith et al. (2018) is 2.6 Wm².

3.2 Positive water feedback

Positive water feedback is a cornerstone in any GCM and the simple model of IPCC. IPCC (2007) writes in AR4 that *“The positive water feedback doubles the radiative forcing of any GH gas.”* The AR5 (IPCC, 2013, p. 667) writes *“Therefore, although CO₂ is the main control knob on climate, water vapour is a strong and fast feedback that amplifies any initial forcing by a typical factor between two and three.”* Because it is a big difference between factors two and three, IPCC should show at least a few references to the proper research studies.

The theoretical justification of positive water feedback is based on the equation of Clausius–Clapeyron. This equation represents the pressure-temperature relationship in a saturated water vapor atmosphere. The real atmosphere is not saturated by water vapor, and therefore the theoretical basis is weak. Because the atmosphere's saturation is around 70% on average, it could possible that the positive water feedback relationship would follow the Clausius–Clapeyron equation. The direct humidity and temperature measurements from 1980 onward show no positive water feedback in the long run.

The encompassing satellite temperature measurements were introduced in 1979 (UAH, 2017). In the same year, a new humidity semiconductor sensor technology Humicap® was introduced by the leading humidity measurement company Vaisala. Reliable empirical conclusions about the water feedback can be drawn from the behavior of the climate since 1979. Global humidity data is available from 1948 but its accuracy is not at the same level as data after 1979.

The temperature according to the UAH satellite data set of the lower troposphere (UAH, 2022) and absolute humidity as Total Precipitable Water (TPW) values from NOAA's NCEP/NCAR Reanalysis dataset (2022) are depicted in Fig. 1. The short-term temperature changes are distinctly related to the El Niño and La Niña events, which are caused by the regional changes of the ocean currents and winds in the tropical central and eastern Pacific Ocean. They initiate the temperature change, and the strong change in absolute humidity amplifies the change by a factor of about 100 percent (Ollila, 2020a). It is practically the same as the positive feedback used by IPCC, but can it be found in the long-term trends?

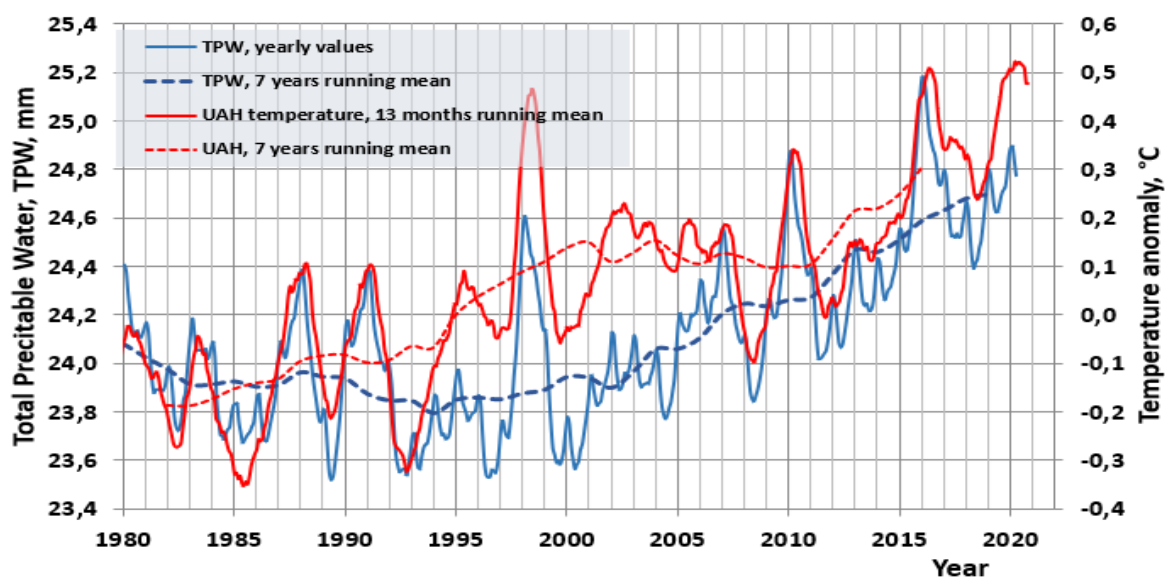


Figure 1. The temperature trend and TPW (Total Precipitable Water) trends from 1980 to 2020.

There are essential features in the long-term trends of temperature and TPW, which are calculated and depicted as yearly and 11-year running mean values. The long-term value of temperature has increased by about 0.4 °C from 1979 to 2000 but the TPW values show a negative trend. During the temperature pause from 2000 to 2015, the TPW values show a positive trend. This behavior of TPW conflicts with the positive water feedback theory.

The surface temperature values can be calculated using a simple equation, as defined by the IPCC (2013, p. 664):

$$dT_s = \lambda * RF [^{\circ}C] \quad (2)$$

where dT_s is the global mean surface temperature change, and λ is the “climate sensitivity parameter”. The IPCC reported in TAR (2001) that “ λ is the nearly invariant parameter (typically about $0.5 \text{ K}/(\text{Wm}^{-2})$.” This λ value was taken from the study of Ramanathan et al. (1985), based on eight research papers varying from $0.47 \text{ K}/(\text{Wm}^{-2})$ to $0.53 \text{ K}/(\text{Wm}^{-2})$. When Syuruko Manabe was awarded the Nobel Prize for Physics in 2021, one of Manabe’s main credits was that he was the first to introduce positive water feedback in 1967 (Manabe, 1967). He concluded that water feedback doubles the original RF of CO_2 , and his λ value was $0.53 \text{ K}/(\text{Wm}^{-2})$. This feature became one of the essential features of GCMs as early as the 1980s but in his original paper, Manabe did not conclude if positive water feedback should be used or not in warming calculations.

In AR6 (IPCC, 2021) the IPCC changed its nomenclature and used the term “climate feedback parameter” α , which is the reciprocal of $\lambda = 1/\alpha$. The feedback parameter α can be decomposed into different types of feedback, and the sum of feedback parameters is the direct relationship between the ERF and the global equilibrium surface temperature change.

Even though the IPCC did not report a λ value for ERF in AR6, it can be calculated from the data in Fig. 7.6 and Fig. 7.7 of AR6 (IPCC, 2021), which are based on the GCM calculations. The ERF value of 2.70 Wm^{-2} results in a warming of $1.27 \text{ }^{\circ}\text{C}$, meaning the λ value of $1.27 \text{ }^{\circ}\text{C} / 2.70 \text{ Wm}^{-2} = 0.47 \text{ }^{\circ}\text{C}/(\text{Wm}^{-2})$, which is applicable in TCR calculations since the λ value of CO_2 is the same.

This λ value means that water feedback has been applied in the GCMs used for calculating warming values in Fig. 7.7.

It is possible to calculate the value of λ using different methods. The simplest method is based on the total energy balance of the Earth by equalizing the absorbed and emitted radiation fluxes (Schlesinger, 1986; Ollila, 2014)

$$SC(1-\alpha) * (\pi r^2) = sT^4 * (4\pi r^2) \text{ [W]} \quad (3)$$

where SC is the solar constant ($\sim 1360 \text{ Wm}^{-2}$), α is the total albedo of the Earth, s is the Stefan-Boltzmann constant ($5.6704 \cdot 10^{-8} \text{ [Wm}^{-2}\text{K}^{-4}]$), and T is the temperature (K). The term $SC(1-\alpha)/4$ is the same as the net radiative forcing (RF) and therefore Eq. (3) can be written in the form $RF = sT^4$. When this equation is derived, it will be $d(RF)/dT = 4sT^3 = 4(RF)/T$. The ratio $d(RF)/dT$ can be inverted, transforming it into λ :

$$dT/(d(RF)) = \lambda = T/(4RF) = T/(SC(1-\alpha)) \text{ [K/Wm}^{-2}] \quad (4)$$

Using the average radiation CERES (2021) flux values for the period 2008–2014, $\lambda = 255.294 \text{ K} / (1360.04 \cdot (1-0.2916) \text{ Wm}^{-2}) = 0.265 \text{ K/(Wm}^{-2})$. Temperature 255.294 corresponds to the Stefan-Boltzmann temperature for radiation 240 Wm^{-2} . Since λ gives the slope of a very nonlinear expression, there might be doubts if temperature change depends linearly closely enough on the RF in the range of about $+10 \text{ Wm}^{-2}$ as needed in the Shared Socioeconomic Pathways (SSP) scenario calculations of the IPCC. In Fig. 2, the emission temperature is depicted as a function of the Stefan–Boltzmann law and according to Eq. (1), using the λ value of 0.265 Wm^{-2} . The deviation between these two curves is insignificant, and the numerical values show that in the RF range from 230 Wm^{-2} to 250 Wm^{-2} , the error with these two equations is only $0.05 \text{ }^\circ\text{C}$. This means that the linear Eq. (1) using a constant λ value is sound when calculating the dT values of different RF forcings.

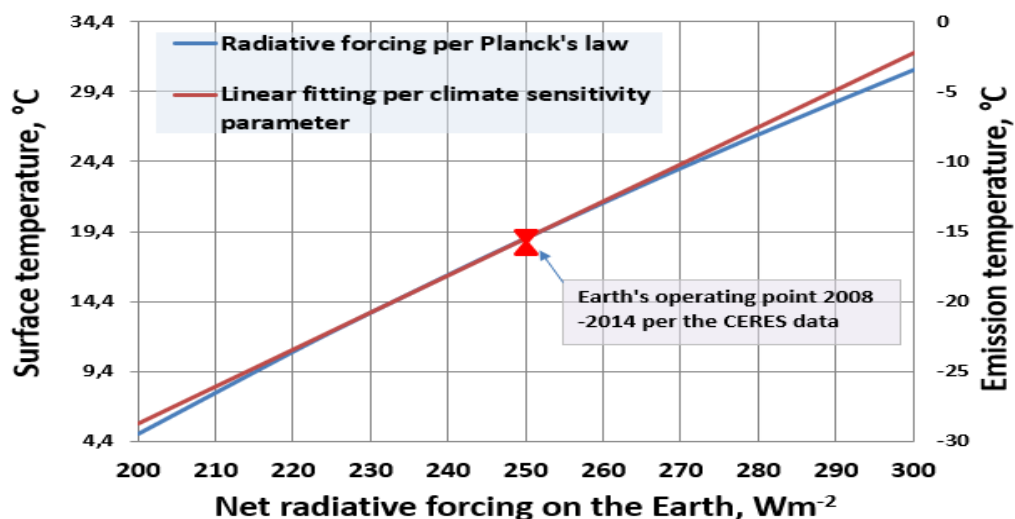


Figure 2. Emission temperature dependency according to Stefan-Boltzmann law and according to linear dependency per Eq. (4).

The difference between the λ values of $0.47 \text{ K/(Wm}^{-2})$ and $0.265 \text{ K/(Wm}^{-2})$ is due to the positive water feedback.

3.3 Climate sensitivity

Climate sensitivity (CS) is a useful measure, telling us how much the Earth's surface temperature T_s would increase driven if CO_2 concentration would increase from 280 ppm to 560 ppm ($=2 \times \text{CO}_2$). There are two types of climate sensitivity, namely Transient Climate Response (TCR) which was called earlier Transient Climate Sensitivity (TCS), and Equilibrium Climate Sensitivity (ECS) (IPCC, 2013). According to AR6 (IPCC, 2021) the "TCR is a surface temperature response for the hypothetical scenario in which atmospheric carbon dioxide (CO_2) increases at $1\% \text{ yr}^{-1}$ from pre-industrial to the time of a doubling of atmospheric CO_2 concentration (year 70)". The TAR of the IPCC (2001) defines TCR as a transition of the surface-troposphere system from one equilibrium state to another.

In the ECS calculations, the climate system must reach the equilibrium, which takes a longer amount of time, because the deep oceans are included and they have a long time to heat up and not all feedbacks are developed into full effects, like albedo changes of the surface for example. IPCC (2013, p. 1112) also states that "TCR is a more informative indicator of future climate than ECS". Therefore, the analyses of this study have been carried out only for TCR values.

Applying Eq. (2) gives the TCR value of $1.85 \text{ }^\circ\text{C}$ ($= 0.47 \text{ }^\circ\text{C}/(\text{Wm}^{-2}) * 3.93 \text{ Wm}^{-2}$), while the best estimate of AR6 (IPCC, 2021) is $1.8 \text{ }^\circ\text{C}$. For example, the T_s for the worst-case scenario SSP5-8.5 determined according to Eq. (1) would be: $dT_s = 0.47 \text{ K}/(\text{Wm}^{-2}) * 8.5 \text{ Wm}^{-2} = 4.0 \text{ }^\circ\text{C}$ using the λ value of the AR6. T_s would be $4.5 \text{ }^\circ\text{C}$ using the λ value of $0.5 \text{ K}/(\text{Wm}^{-2})$, which is practically the same as the average value of $4.4 \text{ }^\circ\text{C}$ of the AR6 calculated by GCMs. These examples show that the average warming values calculated using Eq. (1) are the same as the results calculated by complicated GCMs applicable for the present-day warming, TCR calculations, and scenarios according to SSP (Shared Socioeconomic Pathways) calculations.

This fact is not easily accepted by those researchers who think that these calculations can be correctly carried out only by GCMs. What is the relationship between the λ and the TCR, and are the TCR values calculated using λ close enough to TCR values as defined by the IPCC?

It is a question about the dynamic delays in T_s calculations. The TCR specification (IPCC, 2021) defines that CO_2 increases at $1\% \text{ yr}^{-1}$, from pre-industrial levels to double the atmospheric CO_2 concentration. Since the CO_2 growth rate has been smaller than $1\% \text{ yr}^{-1}$, the dT effects from 1750 to 2019 in Figure 7.7 of AR6 can be simply calculated according to the equation $T = \lambda * \text{RF}$. This means that the results are the same when using Eq. (1) compared to the average results of several GCM simulations. The same applies to TCR calculations, as shown above: $1.85 \text{ }^\circ\text{C}$ using λ versus $1.8 \text{ }^\circ\text{C}$ using GCMs. If there were time delays in response longer than one year, the equation $dT = \lambda * \text{RF}$ would give different results.

One could expect, that the TCR values calculated by GCMs are more accurate than those calculated by using Eq. (1). In fact, there is quite a significant uncertainty range by using GCMs as can be found in the AR6 (IPCC, 2021): "The best estimate of TCR is 1.8°C , the likely range is 1.4°C to 2.2°C ". This uncertainty comes from the GCMs, which use different modeling methods and especially different amounts of various feedback. It means that GCMs do not improve the accuracy of TCR calculations but increase uncertainty for the reasons commented above.

Using Eq. (1) for calculating the warming values is correct since the dynamical time constant for the ocean is 2.74 months, and for land, 1.04 months (Stine et al., 2009). These values mean that for a stepwise RF change, T_s has reached its new equilibrium value in one year, since the settling (relaxation) time is about four times longer (98.3 % of the final change achieved) than the

residence time ($4 * 2.74 = 11$ months) according to a first-order process dynamic system having a single time constant.

The literature survey of non-IPCC TCR values can be divided into three major categories based on the research method, namely A) using the $2*CO_2$ values of the IPCC, B) using the $2*CO_2$ by applying researchers own LBL analysis calculations, C) using observed Ts values and other climate data.

The survey of research studies of category C reveals that the TCR values vary from 0.0 °C of Fleming (2018) to 1.2 °C of Otto et al. (2013). The results of this category are not reliable enough since they are too heavily dependent on other climate drivers like solar irradiation variations, volcanic impacts, surface albedo changes, etc. Kissin (2015). Usually, the elimination of these effects has not been considered at all.

The TCR values of category A are very consistent since they are very close to each other: 1.15 °C from Bengtson and Schwartz (2012), 1.2 °C from Schlesinger (1986), and 1.33 °C from Lewis and Curry (2015). Even though these research studies apply 3.7 Wm^{-2} as the RF value, they have not found positive water feedback in the climate explaining the deviations from the IPCC's value of 1.8 °C. These results are fully in line with the IPCC (2007), which writes in section 8.6.2.3 of AR4 that "*with any feedback operating, the global warming from GCMs would be around 1.2 °C.*" Ollila (2020b) has carried out warming calculations by applying only feedback from the atmosphere, which is called Planck's response. Using an RF value of 3.7 Wm^{-2} gives the warming value of 1.12 °C, which is also very close to the values above.

The results of category B vary considerably little: 0.6 °C by Barrett et al. (2006), 0.48 °C by Miskolczi and Mlynczak (2004), 0.51 °C by Ollila (2012), 0.6 °C by Ollila (2014), 0.5 – 0.7 °C by Kissin (2015), 0.4 °C by Smirnov (2017), 0.7 °C by Harde (2017), and 0.5 °C by Schildknecht (2020). The only explanation is that these researchers have found a smaller $2*CO_2$ value than 3.7 Wm^{-2} and they have not found positive water feedback. The differences cannot be explained by the identified flaws in calculation methods.

It should be noticed that the survey of this study does not cover all research studies showing lower CS values than IPCC. Gervais (2021) has listed 109 studies that conclude that CS is from 0.0 to 1°C. The most common result of these studies is that the TCR/ECS value is negligible or close to zero, and they are usually based on the analysis of empirical climate data. The studies of Miskolczi (2014) and Drotos et al. (2020) have proposed a feedback mechanism in the climate that will drive the long-term temperature effect of $2*CO_2$ to zero, which means that the GH effect would be constant and not depend on the CO_2 concentration; so far, these proposals have not received any common acceptance.

3.4 Relative strengths of major GH gases

The global warming potential (GWP) definition means how much a GH gas can absorb infrared energy if 1 kg has been released into the atmosphere over a specified period (normally 100 years) when compared to the same amount of CO_2 gas (IPCC, 2007). The 100-year GWP value of methane is 27.9 and the same value of nitrogen oxide is 273 (IPCC, 2021). The GPW value definition is highly theoretical, and it is not applicable in warming calculations, because only the actual GH gas concentration has a warming impact and not the future concentrations.

A more realistic analysis can be carried out to find out the relative strengths in the climate of this century by increasing the GH gas concentration in question by 10 % from its concentration in the present atmospheric conditions and calculating the absorption for the altitude of 120 km (Ollila, 2017a). When CO_2 acts as a reference having a strength of 1, the relative strengths of other GH

gases are water 11.8, ozone 0.78, nitrogen oxide 0.14, and methane 0.11,

The simplest method for comparing the relative strengths of GH gases is to compare their RF values from 1750 to 2019 as shown in Table 1.

Table 1. Relative strengths of carbon dioxide, methane, and nitrogen oxide according to AR6 (IPCC, 2021, Fig. 7.6) based on the concentration changes from 1750 to 2019.

GH gas	RF in 2019, Wm ⁻²	Concentration change, %	RF/1% change	Relative strength
CO ₂	2.16	40.36	5.35	1
CH ₄	0.54	159.17	0.34	0.11
N ₂ O	0.21	20.00	1.05	0.25

These two calculation methods show that the GWP values give wrong images about the strengths, and they do not represent the warming impacts of GH gas on a certain year during this century. The warming impact of water is almost linearly dependent on the water vapor content in the atmosphere, and it explains why water is such a strong GH gas.

The physical explanations for these relative strengths can be noticed in Fig. 3, where the absorption peaks of major GH gases have been depicted.

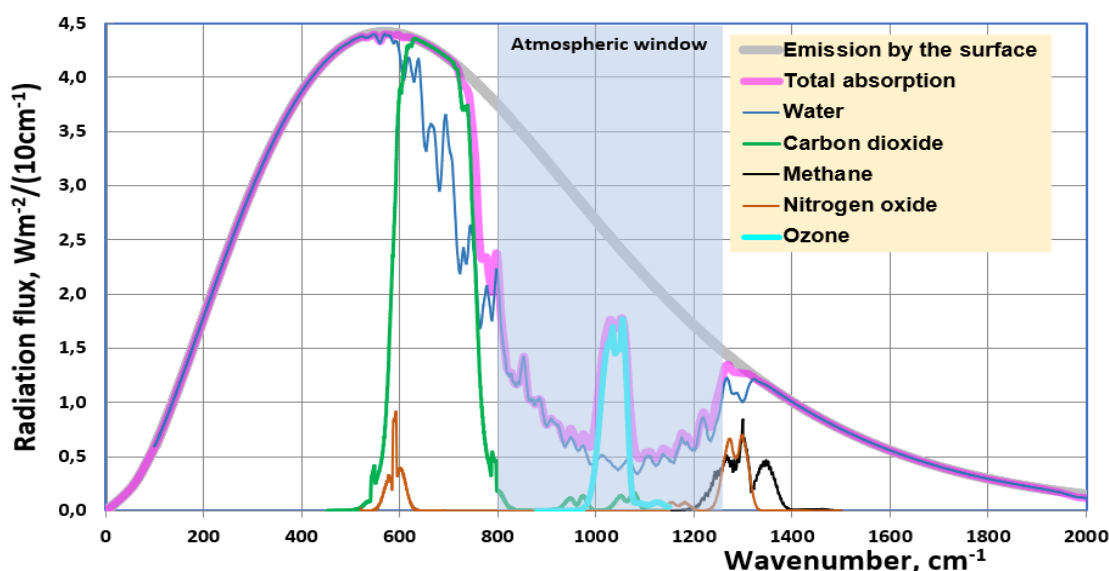


Figure 3. The absorption areas of GH gases in clear sky conditions.

The absorption peaks of methane and nitrogen oxide are badly overlapping with the absorption effects of water and carbon dioxide explaining their weak RF impacts. On the other hand, the absorption peak of ozone is relatively strong since its absorption wavenumber zone from 1000 to 1100 water has the minimum absorption effect.

3.5 Carbon dioxide circulation and time delays in the atmosphere

In calculating the future warming impacts of CO₂, it is important to know in which way fossil emissions would change the atmospheric CO₂ concentration. The only way to find out this behavior is to build a model simulating the carbon cycle between the atmosphere, the ocean, and the land. About 25 % of the atmospheric CO₂ changes every year, because the oceans absorb and dissolve CO₂, and in the same way land plants (later land) photosynthesize and respire CO₂. The present-day anthropogenic emission of about 10 GtC per year (gigatons of carbon) is only 4.5 % of the annual CO₂ flux of about 220 GtC circulating through the atmosphere.

Since 1960, CO₂ circulation has behaved practically the same way that about 55 % of annual emissions have been taken up by the two sinks. During the last 10 years, the atmospheric CO₂ amount has increased yearly with the amount corresponding to about 4.5 GtC, which is 45 % of the annual fossil fuel emissions but it does not mean that this increase is totally anthropogenic as the IPCC assumes. Yearly fossil emissions mix with the existing atmospheric CO₂. From this almost evenly mixed CO₂, the ocean, and the land uptake CO₂ according to their atmospheric composition, and simultaneously CO₂ flows into the atmosphere from the ocean and the land having different compositions. A comprehensive isotope measurement study of the dissolved CO₂ in the ocean (Sabine et al., 2004) shows that the ocean is a sink for anthropogenic CO₂, but the sink of the total CO₂ (total CO₂ is the mixture of anthropogenic and natural CO₂) between the ocean and the land is not clear. The ocean used to be the main sink for the total CO₂ (IPCC, 2013; Ollila, 2020c) before 1960. According to the AR6 (IPCC, 2021) during 2010-2019 the average yearly sink anthropogenic CO₂ value of 5.9 GtC yr⁻¹ was divided 42 % versus 58 % between the ocean and the land. This means that if the recycling system of CO₂ works in the same way also during this century, the atmospheric CO₂ concentration will increase steadily.

Two permanent isotopes of carbon molecules exist. The most common is ¹²C, having 6 protons and 6 neutrons; however, ¹³C has one extra neutron. Isotope ¹²C is the most common, being 98.9 % of all carbon; the rest is ¹³C. An exceedingly small concentration of unstable isotope ¹⁴C, which is radioactive, also exists.

The measurement unit of ¹³C (marked as δ¹³C) is a fraction of carbon isotope ¹³C expressed as ‰, and it has been called permille. This unit is linearly dependent (Srivastava et al., 2018) on the relationship ¹³C/¹²C:

$$\delta^{13}\text{C} = (\text{S/N}-1) * 1000 [\text{‰}] \quad (5)$$

where S = ¹³C/¹²C being a sample and N = (¹³C/¹²C)_{standard} = 0,0112372. The value of the standard comes from a sea fossil “Belemnitella Americana.” Many climate researchers have never heard about this measurement unit. It looks like the IPCC does not want to report on permille values since in the AR6 (IPCC, 2021) is only one figure namely Fig. 5-6 and its panel c, where is a short permille trend of the atmospheric CO₂. The same applies to the main referred research study (Friedlingstein et al., 2020), which is the basis of the carbon cycle description in the AR6: no reference to the permille values.

Anthropogenic CO₂ means CO₂ originating from fossil fuels and land use (NOAA, 2018). Fossil fuels have the same permille value as plants from the Carboniferous era (359 – 299 million years ago); this value is -28 ‰. The typical δ¹³C values in the present day are the atmosphere about -8.6 ‰, the ocean surface from -8.0 ‰ to -10 ‰, the land -26 ‰, and the fossil fuels -28 ‰ (Quay et al., 2003; NOAA, 2020c).

The permille unit is odd because most values of carbon dioxide (CO₂) mixtures are negative. The atmosphere is the mixture of natural CO₂ from the ocean and plants and the fraction of anthropogenic emissions remaining there. The term “total CO₂” has been used for the mixture of natural and anthropogenic CO₂ flux or amount. The Suess Effect shifts continuously the isotopic ratio of both ¹³C and ¹⁴C in the atmosphere and the ocean because of anthropogenic CO₂ emissions. The change in δ¹³C value is mainly due to the combustion of fossil fuels and the circulation of CO₂. Because the permille values of anthropogenic CO₂ differ so much from the atmospheric values today (-8.6 ‰), it can be used to calculate the fraction of anthropogenic CO₂ in the atmosphere by applying carbon circulation models.

Carbon cycle models referred to by the IPCC are all-encompassing and they apply several sub-models designed for special tasks like CO₂ exchange with plants. In this section, the approach is to analyze critically the IPCC’s carbon cycle model, which refers to the yearly published article “Global Carbon Budget” by Friedlingstein et al (2020), and to compare its key figures to the results of the 1DAOBM-3 model of Ollila (2020c), and Berry (2021).

In AR5, the IPCC (2013a, p. 467–469) writes: “*About half of the emissions remained in the atmosphere 240 PgC±10 PgC since 1750.*” In the same way in AR6 (2021), the increased mass of the atmosphere originates from the emissions. The total CO₂ mass in 2019 was 876 GtC; in 1750, the same was 591 GtC (IPCC, 2021). Two simple tests can be carried out to check the numbers of the AR6. If all the CO₂ increase were anthropogenic CO₂ as IPCC reports (2021), its amount would be 285 GtC in 2019, meaning a fraction of 32.5 %. The rest (67.5 %) would be assumed to be natural CO₂ having a δ¹³C value of -6.35‰, which is the permille value of the atmospheric CO₂ in 1750. The δ¹³C of this atmospheric CO₂ mixture would be

$$\delta^{13}\text{C} = 0.324 * (-28) + 0.676 * (-6.35) = -13.4 \text{ [‰]} \quad (6)$$

If eq. (6) would give the permille value of -8.6 ‰, the permille value of the natural CO₂ in the atmosphere should be about +1.0 ‰. Since the plants have not been sink according to AR6 (IPCC, 2021, p. 5-22), the land has not changed the atmospheric permille value. The ocean has been the major sink but the fractionation from air to sea and from sea to air are so close to each other that the recycling fluxes have not been able to change the natural CO₂ value significantly. This analysis shows that the increased atmospheric mass from 1750 cannot be totally anthropogenic since the currently observed δ¹³C is about -8.6‰.

Another test can be carried out to test the correctness of the carbon cycle figures of the IPCC (2021). There is a fractionation phenomenon from air to sea, from sea to air, and vegetation CO₂ exchange. However, about 99 % of anthropogenic CO₂ is a carbon isotope of ¹²C; therefore, its recycling happens similarly to natural CO₂. Although the ¹³C fraction would differ in recycling anthropogenic carbon fluxes, over 99 % is the same material, which must still be labeled anthropogenic if it originates from human actions. Table 2 has enlisted the carbon cycle fluxes (CCFs) of the IPCC (2021) from Fig. 5.12 since it is the only presentation of this kind in the AR6.

Table 2. The average CCFs (GtC yr⁻¹) from 2010 to 2017, according to IPCC (2021, Fig. 5.12), and the percentage fraction of the anthropogenic CO₂ from the total oceanic or terrestrial CCF.

Total carbon cycle flux from the atmosphere, GtC yr ⁻¹	Anthropogenic CO ₂ and percentage from the CCF
Total CO ₂ in the atmosphere, 870 GtC	279 GtC, 32.1 %
From the atmosphere to the ocean, anthropogenic, 79.5	25.5 GtC yr ⁻¹ , 32.0 %
From the atmosphere to land plants, anthropogenic, 142.0	29.0 GtC yr ⁻¹ , 20.4 %

The key figures in Table 2 mean that the ocean-atmosphere flux would not discriminate the atmosphere’s anthropogenic fraction since it contains the same 32.0 % of this fraction because in the atmosphere this fraction is the same of 32.1 %. Surprisingly enough, the gross photosynthesis flux has only 20.4 % of anthropogenic CO₂. Does a physical explanation for this land discrimination exist? No. Instead, the plants prefer anthropogenic CO₂ for its higher ¹²C isotope concentration. The ocean’s euphotic layer (max. depth of about 200 m) also favors anthropogenic CO₂ since phytoplankton and plants prefer the ¹²C.

According to the IPCC (2021), when there is an annual emission of anthropogenic CO₂ increase,

only the anthropogenic molecules will be sequestered by the sea and the land plants, and on average 44-45 % is removed from the atmosphere annually (IPCC, 2021). Both anthropogenic and natural CO₂ has about 98.9 % carbon isotopes ¹²C, but there is no natural process that could identify the origin of ¹²C and select only ¹²C molecules with the anthropogenic origin, which would be sequestered and not a single one with a natural origin. In reality, sequestration of ¹²C must happen according to the relative amounts of these molecules: if the concentration of ¹²C with the natural origin is double in comparison to anthropogenic ¹²C molecules, the double amounts will be sequestered.

The fractionation phenomenon between the reservoirs changes the relative amounts of ¹³C molecules (amount only about 1.1 %) and it affects the permille number of the CO₂ amount sequestered by a reservoir. But fractionation does not control the sequestration process since it is only a consequence.

According to AR6 (IPCC, 2021), “*The ocean uptake of anthropogenic carbon is a two-step set of abiotic processes that involves the exchange of CO₂, first across the air-sea boundary into the surface mixed layer, followed by its transport into the ocean interior where it is stored for decades to millennia, depending on the depth of storage (Gruber et al., 2019).*” This adiabatic process means that the atmospheric CO₂ dissolves in the surface ocean according to Henry’s law, which leads to the equilibrium between the atmospheric and the dissolved CO₂. The study of Humlum et al. (2013) reveals that the time lag between CO₂ concentration changes and the ocean’s surface temperature is 11-12 months globally.

The AR6 (IPCC, 2021) does not report, in which way the anthropogenic CO₂ is divided between the ocean mixing layer and the intermediate & deep ocean. Gruber et al. (2019) reported that 50 % of the anthropogenic CO₂ is in the layer above 400 meters depth. The total anthropogenic CO₂ in the ocean was 160 GtC in 2019 (IPCC, 2021). Since the surface mixed layer depth is 75-100 meters, the anthropogenic CO₂ in this layer can be estimated to be about 0.3*0.5*160 = 25 GtC. According to IPCC (2021), the annual average recycle 2008-2017 flux of anthropogenic CO₂ was 25.5 GtC. These figures would mean that the ocean recycle flux would return yearly into the atmosphere practically all the anthropogenic CO₂, which was absorbed by the surface mixed layer. This would mean zero sequestration rate by the ocean. This is another example of the physical contradictions of the IPCC model.

The main differences in carbon cycle representations between the AR6 of the IPCC (2021), which is based on the research report of Friedlingstein et al. (2020), Ollila (2020c), and Berry (2021) have been tabulated in Table 3.

Table 3. The key figures of anthropogenic CO₂ according to Friedlingstein et al. (2020) from 2010 to 2019, Ollila (2020c) for the year 2019, and the same of Berry for the year 2020.

Reservoir	Cumulative 1750-2019			Yearly net fluxes	
	IPCC	Ollila	Berry	IPCC	Ollila
Amount (GtC) or flux (GtC yr ⁻¹)					
Anthropogenic CO ₂ in/to the atmosph.	285	70	71	5.1	0.3
Anthropogenic CO ₂ in/to the ocean	170	250	206	2.5	5.8
Anthropogenic CO ₂ in/to land plants	230	166	71	3.4	3.2
Total anthropogenic amount, GtC	685	486	452		

The total amount of anthropogenic CO₂ of Ollila includes 32 GtC of land-use CO₂ emissions, and the same of the IPCC is 240 GtC (imbalance in terrestrial sink 10 GtC). The anthropogenic CO₂ amounts of Berry and Ollila are very close to each other, and the main difference is due to the land-

use emissions applied by Ollila. This result is very interesting since the calculation basis of Ollila is a complicated model of CO₂ recycling between different reservoirs considering the fractionation between reservoirs and Berry's approach is simpler.

The ocean absorbs anthropogenic CO₂ yearly at 5.8 GtC according to Ollila (2020c) but in the IPCC's model, it is only 2.6 GtC. The anthropogenic flux 5.8 GtC yr⁻¹ is not the net absorption rate of total CO₂, since there is a natural CO₂ flux of 3.6 GtC yr⁻¹ back into the atmosphere keeping the net sequestration rate in 2.2 GtC, which is less than in buffer-factor models (2.6 GtC yr⁻¹). This is the reason for the composition of the total atmospheric CO₂ increase of 265 GtC since 1750: 195 GtC of natural CO₂ and 70 GtC of anthropogenic CO₂.

According to Friendlingstein et al. (2020) and the IPCC (2021), the amount of 265 GtC is totally anthropogenic by nature. This is an assumption, which has not been supported by any figures or analyses. In AR4 the IPCC (2007, p. 948) says that the turnover time for natural CO₂ is about four years. It is in line with the definition of the turnover time, which is calculated by dividing the total CO₂ mass of the atmosphere mass of 880 GtC with a total CCF of 220 GtC yr⁻¹, which gives the same figure. In AR5 the IPCC (2013, p.469) writes: "The removal of human-emitted CO₂ from the atmosphere by natural processes will take a few hundred thousand years (high confidence). Depending on the RCP scenario considered, about 15 to 40% of emitted CO₂ will remain in the atmosphere longer than 1,000 years." This is again an example of the physical contradictions of the IPCC carbon cycle model.

In tracer testing, which is commonly used in scientific studies, a very small amount of a chemical or a radioactive compound is used to detect flows, delays, and other dynamic properties of a fluid system under scrutiny. For estimating the residence time of the anthropogenic CO₂ in the atmosphere, the results of the only full-scale test carried out by humanity with the climate are now available. The nuclear bomb tests in the atmosphere from 1945 to 1964 accidentally created this kind of tracer test situation.

The decay curve of the ¹⁴C can be combined with some of the worldwide measurements (Levin et al., 2010; Utrecht, 2016; LLNL, 2016) carried out since the 1950s and this is illustrated in Fig. 4. The simulated decay rate of the first order dynamic system with a residence time of 16 years gives an excellent fit.

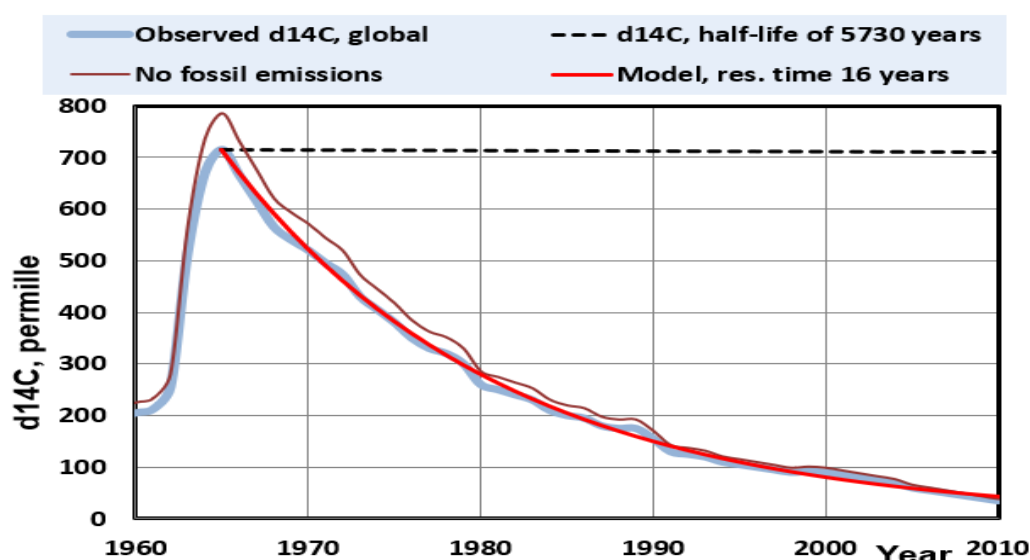


Figure 4. The observed global decaying rate of ¹⁴C (blue curve), the simulation result by 1DAOBM-3 (red curve), the theoretical decaying rate of ¹⁴C without recycling fluxes in the carbon circulation system (black dashed curve), and the estimated decaying rate in the climate system without fossil fuel emissions (brown curve).

This tracer test by the ^{14}C corresponds perfectly to the behavior of anthropogenic CO_2 . In both cases, the concentration change of a new CO_2 flux into the atmosphere starts from zero. The nuclear bomb test can be used to validate any CO_2 circulation model.

If a model gives a shorter residence time of 16 years for anthropogenic CO_2 in the atmosphere, it is probably wrongly composed. This is true for early research studies showing residence times from 2 to 15 years, which gives an average residence time is 7.6 years, which was identified by Segalstad (1998) when he surveyed 34 residence time studies from 1957 to 1990. A common feature of these studies is that they have used a model, where is one mixing tank (the atmosphere) and the total CCF flows through this tank. This process model is flawed since in reality, the carbon cycle encompasses three reservoirs with recycling fluxes.

Revelle and Suess (1956) estimated that “the exchange time” for an atmospheric CO_2 molecule to be absorbed by the sea is “the order of magnitude of 10 years”. In this case “the exchange time” T_e was defined to be the half-life time since T_e was marked to be $1/k$, where k is the time constant of the first-order dynamic system. A half-time means the time when 50 % of the change has happened. For the first order system a half time = $\ln 2/k = 0.693/k$. Residence time T (also called turn-over time) is $1/k$. Therefore, in the first order system $T_e = 0.693 * T$.

The value of 10 years of T_e by Suess and Revelle corresponds to 14.4 years of residence time. This value calculated from cosmogenic ^{14}C data is surprisingly close to 16 years of T confirmed by the empirical nuclear bomb tracer test years later.

Another useful timescale is relaxation time or adjustment time (marked with T_{adj}), which means the time needed for a perturbed system to return to equilibrium or a steady state. Because theoretically, T_{adj} would be infinitely long, in practice T_{adj} is approximated by multiplying the residence time by four: $T_{\text{adj}} = 4 T$. At this time moment, a step change has reached the level of 98.3 % from the final equilibrium value. The IPCC uses T_{adj} values in reporting how long it takes the anthropogenic CO_2 to leave the atmosphere if anthropogenic emissions would stop.

The conclusion about IPCC’s adjustment time for anthropogenic CO_2 is that it is in direct conflict with the tracer test results with radiocarbon. The relaxation time of 1DAOBM-3 is 64 years is the same as the radiocarbon relaxation time.

The simulation results applying 1DAOBM-3 (Ollila, 2020c) and Berry (2021) show that the amount of the anthropogenic CO_2 in the atmosphere in 2019 is only 70 GtC, corresponding to the portion of 8 % because natural CO_2 flows into the atmosphere from the ocean and the vegetation. According to Ollila (2020c), this amount is concordant with the $\delta^{13}\text{C}$ measurement in 2017 (Locean, 2016) being -8.6 ‰. Any permille value observation or presentation and how it should be calculated cannot be found in the AR6 (IPCC, 2021) or Friedlingstein et al. (2020). The conclusion could be that the division between natural and anthropogenic atmospheric CO_2 amounts does not support the observed $\delta^{13}\text{C}$ value.

Harde and Salby (2021) have concluded that the residence times of atmospheric natural and anthropogenic CO_2 are the same since the CO_2 molecules are similar. They use the term “absorption time”, which seems to be according to graphical presentations the same as the residence time of 16 years of bomb carbon.

A simple test can be carried out if the adjustment time of 64 years could be possible for the total CO_2 increase of 285 GtC from 1750 to 2019. How long it would take that the extra 285 GtC in the atmosphere would decrease to zero if the anthropogenic emissions (about 10 GtC yr^{-1}) were stopped totally? If the yearly decrease is the same as the present-day sequestration rate of about 5.5 GtC each year, it would take 52 years. But as the decay curve of ^{14}C shows in Fig. 4, the decay rate will decrease continually according to the first-order dynamic model, which time constant is

16 years. The atmospheric anthropogenic amount of 70 GtC can decrease to almost zero in 64 years as has happened but it is impossible to the total CO₂ amount of 285 GtC due to the restricted sequestration capacity of the ocean and the land plants.

The only way to find an answer is a model simulating carbon recycling between the three reservoirs. Ollila has simulated the decrease rate of the total atmospheric CO₂ when anthropogenic emissions stop by applying his model 1DAOBM-3 and the simplified dynamic models of Bern2.5CC (Joos et al., 2001) and Joos2013 by Joos et al. (2013). Bern2.5CC has been also the selection of the IPCC. The results have been depicted in Fig. 5.

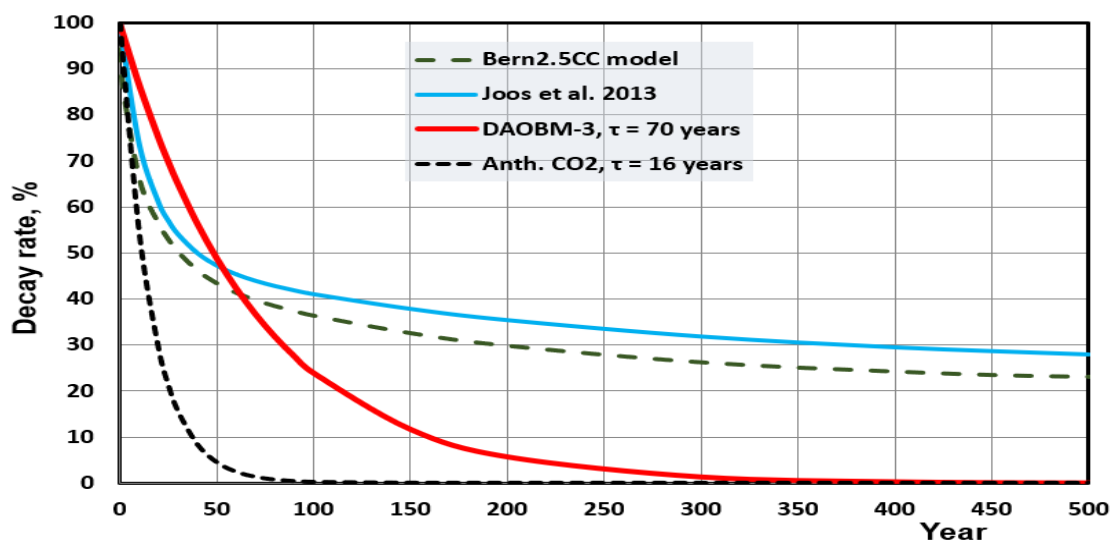


Figure 5. Decay rates of total atmospheric CO₂ concentration using different carbon cycle models, and the anthropogenic CO₂.

The dynamic models of Bern2.5CC and Joos2013 are combinations of four first-order dynamic models with different residence times from 1.189 years to 393.4 years and a constant, which means that CO₂ would never decrease to zero level but stay at the level of about 20 % from the original starting level. There is no physical reason for this assumption.

The fitting of the 1DAOBM-3 simulation shows that a residence time of about 70 years is a reasonable compromise. It is not very good fitting since recycling fluxes, especially from the land, increases on yearly basis more and more CO₂ into the atmosphere. It means that the adjustment time would be $4 \cdot 70 = 280$ years before the atmospheric CO₂ level would have returned to about the same level as 1750. It is not probably a coincidence that the present CO₂ concentration increase has happened during the last 270 years. The surface temperature after 2010 in this simulation has been constant.

A common feature among the IPCC contrarians is that the increase in atmospheric CO₂ cannot be totally anthropogenic since they find several faults and violations of physical laws in the IPCC's carbon cycle modeling. There are still different results among the contrarian research studies but they are closing each other.

3.6 The decadal climate oscillations

The first observational evidence for about 60- to 80-year temperature oscillations in the North Atlantic basin was identified during the 1980s (Folland et al., 1984; Folland et al., 1986), and they

were followed by Schlesinger and Ramankutty (1994), and Klyashtorin et al. (2009). This phenomenon was termed the Atlantic Multidecadal Oscillation (AMO) by Kerr (2000). Chen et al. (2018) identified the same kind of oscillation in the northern part of the Pacific, and it has been termed the Pacific Multidecadal Oscillation (PMO).

Researchers of astrophysics have studied the cyclic behavior of solar magnetic activity since 1843 when it was discovered by Schwabe (1843) to have about an 11-year duration. Hale (1908) discovered the magnetic nature of sunspots and that the complete magnetic cycle spans two solar cycles (22 years). Gleissberg found in 1958 that the solar cycles weaken and strengthen in the period of about 80 years by applying a lowpass filter to the sunspot number records. The periodicity of the 88-year Gleissberg cycle like the 220-year Suess (1980) cycle is related to the Schwabe cycle.

The same periodicities of about 60- to 90-year have been found in regional and global measurements during the thousands of years like the global temperature (HadCRUT5, 2021), Indian monsoons (Agnihotri et al., 2002), NE Pacific coast sediments (Patterson et al., 2004), cosmogenic isotope concentrations of ^{14}C and ^{10}Be (Attolini et al., 1987; Cini Castagnoli et al., 1992), auroral records (Feynman and Fougere, 1984), and tree-ring analyses (Lin et al., 1975; Peristykh and Damon, 2003; Ollila and Timonen, 2022). Scafetta (2010) and Ollila (2017b) have introduced and analyzed the planetary oscillation called Astronomic Harmonic Resonances (AHR), which creates a 60-year oscillation pattern. These different 60-oscillations have been depicted in Fig. 6.

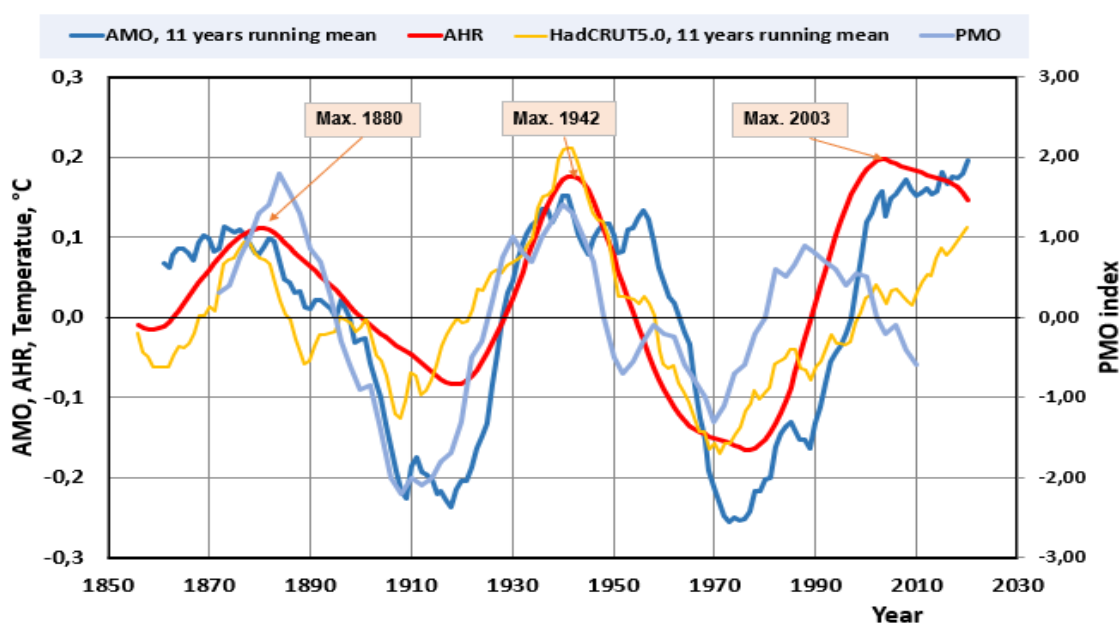


Figure 6. The 60-year fluctuations of AMO (NOAA, 2022), PMO, AHR, and temperature trends. The AHR trend is from the study of Ollila (2017b), and the PMO has been digitized from Fig. 5 of Chen et al. (2016) with 2-year steps.

As Fig. 6 indicates, the AMO and PMO are probably connected to global-scale multidecadal oscillation (GSMO), also called Global-Scale Multidecadal Variability of about 50 to 70 years as observed in the temperature behavior. The trends also illustrate the fact that the NH oscillations are stronger than global oscillation amplitudes.

Internal and external forces have been proposed to cause oscillations. Ermakov et al., (2009) were

the first to introduce that the cosmic dust variations may cause temperature oscillations. Scafetta (2010) and Ollila (2017b) have analyzed that the orbital periods of Jupiter and Saturn can create temperature variations of 60 years by moving the solar system barycentre, which causes variations in the cosmic dust amount entering the atmosphere. The temperature effect happens through cloudiness variations.

Ollila and Timonen (2022) analyzed the year-accurate tree-ring data series called the Finnish Timberline Pine Chronology (FTPC) from the year 1000 onward. They found that the tree-ring variations can be explained with two oscillation periods of 60- and 88-years. The 60-year period matches the AHR phenomenon, and the longer oscillation is a well-known 88-year oscillation, which was first discovered by Gleissberg (1958). This oscillation can be connected to the repetitive occurrence of the basic solar Schwabe cycle of 11 years (varying from 10 to 14 years) as well as the Hale 22-year cycle. In Fig. 6 the 60- and 88-year cycles have been combined and the periodicity of the combined signal correlates very well with the FTPC tree-ring signal, Fig. 7.

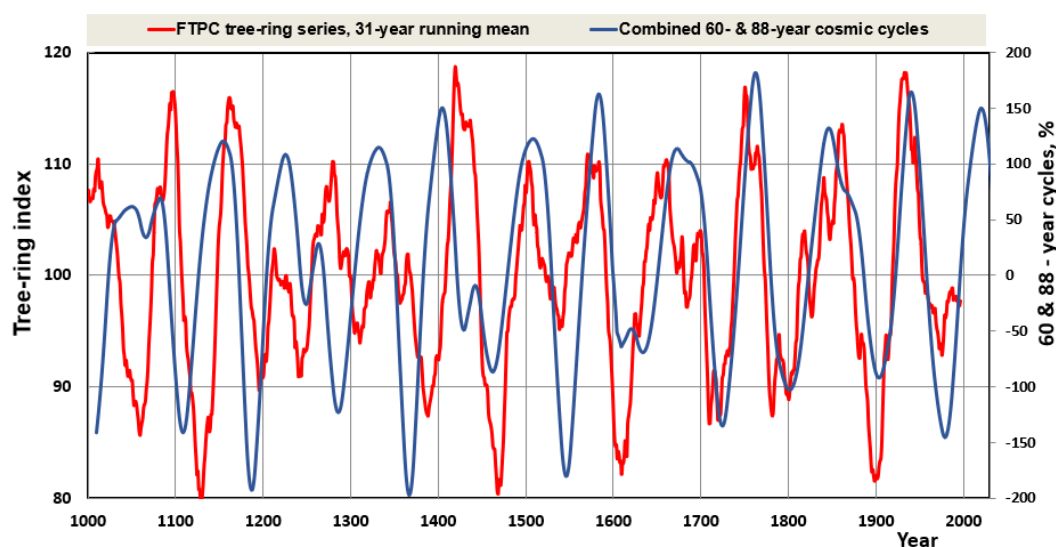


Figure 7. FTPC 31-year running mean signal and combined AHR & Gleissberg signal.

The temperature effect of the 60- & 88-year signal on the temperature change from 1750 to 2019 is minimal since there are grand maximums (simultaneous maximums) during these years. On the other hand, this oscillation can explain the cyclic behavior of the global temperature from 1750 to 2020.

The 60- to 88-year oscillations had their simultaneous maximums in 1940. When the oscillation phases changed to negative phases, the cooling effect of the 60- & 88-year oscillations became dominant over the greenhouse gas effects and caused global temperature to decrease, which happened from 1940 to 1975. Similarly, when the 60- & 88 oscillations turned from a negative to a positive phase, global warming accelerated, as it did after 1975 and finally increased the global temperature by about 0.25 °C (Fig. 6) till 2000. The IPCC has not recognized this temperature behavior in its temperature reconstruction during the 1900s.

3.7 Century- and millennial-scale climate oscillations

Century- and millennial-oscillations have a major role in explaining long-term variations thinking the anthropogenic period from 1750 to the present. If there are longer periodicities than about 250 years, they are possible explanations for the present-time warming at least partially. The first step is to find out research studies analyzing these periods and the second step is to analyze the

proposed mechanisms.

Century- and near-millennium scale research studies have used typically ice-core drilling samples of Antarctica and Greenland, and the other group of studies has used cosmogenic analyses of ^{14}C and ^{10}Be samples from other sources like marine and lake sediment records, and $\delta^{18}\text{O}$ records of speleothems (geological formations of mineral deposits in natural caves).

The analyses (Davis et al., 2017; Davis et al., 2018; Davis et al., 2019) of Antarctica drill hole samples have revealed a dominating periodicity of about 143-146 years during the last 446 millennium years, which has been coined to Antarctic Centennial Oscillation (ACO) and Antarctic Oscillation (AAO). The analyses show also millennial-scale oscillations from 800 to 1500 years.

The temperature and CO_2 variations are smaller in Antarctica than in Greenland, and therefore same oscillations should be easily found also on the Northern Hemisphere. Dansgaard et al. (1984) and Dansgaard et al., (1993) concluded from the ice-core records of Greenland for the period of 250 000 years that climate has been unstable during glaciation periods, and these climate periods were named Dansgaard – Oeschger (D-O) oscillations. The periodicities of Greenland's ice-core records according to Vinther et al. (2010) have been 1270, 1470, and 2550 years. In the later article of Vinther (2011), a dominant period is about 1000 years peaking at 1000 and 2000 years. Bond (1997) has found the same 1470 ± 500 years periodicity in the North Atlantic Sea sediments during the Holocene.

Davis et al. (2019) have named external forces of the Earth like periodic variations in solar insolation and natural perturbations of Earth's orbital cycles to be probable reasons for variations.

Also, Bond (1997) thinks that oscillations found in the North Atlantic area are caused by solar insolation changes.

3.8 The Sun's activity changes

The Earth receives about 99.97 % of its energy from the Sun. The Sun's radiated energy measure is Total Solar Irradiance (TSI), which has both long-term variations in the millennium scale and short-term variations like Schwabe's 11-year cycle and Gleissberg's 88-year cycle. Solar magnetic field variations are responsible for solar irradiation changes. There are two main categories of methods in evaluating historical TSI values, which are sunspot records starting from 1610 and cosmogenic isotopes of ^{10}Be and ^{14}C applicable for millennial periods.

Hoyt and Schatten (1993) have used the indices of the equatorial solar rotation rate, sunspot structure, decay rates of sunspots, the number of sunspots without umbrae, and the decay rate of sunspots and sunspot cycle, and developing a model for TSI calculation. Lean (1995, 2004, 2010) has reconstructed the TSI trend from 1610 onward by using revised sunspot activity records and the correlation between sunspot darkening and faculae brightening (bright areas between sunspots data). Bard et al. (2000) have used the cosmogenic isotope measurements of ice cores samples of the South Pole. Shapiro et al. (2011) and Steinhilber et al. (2012) have found that solar irradiance and cosmic radiation variations have caused large historical solar forcings. These TSI constructions have been depicted in Fig. 8.

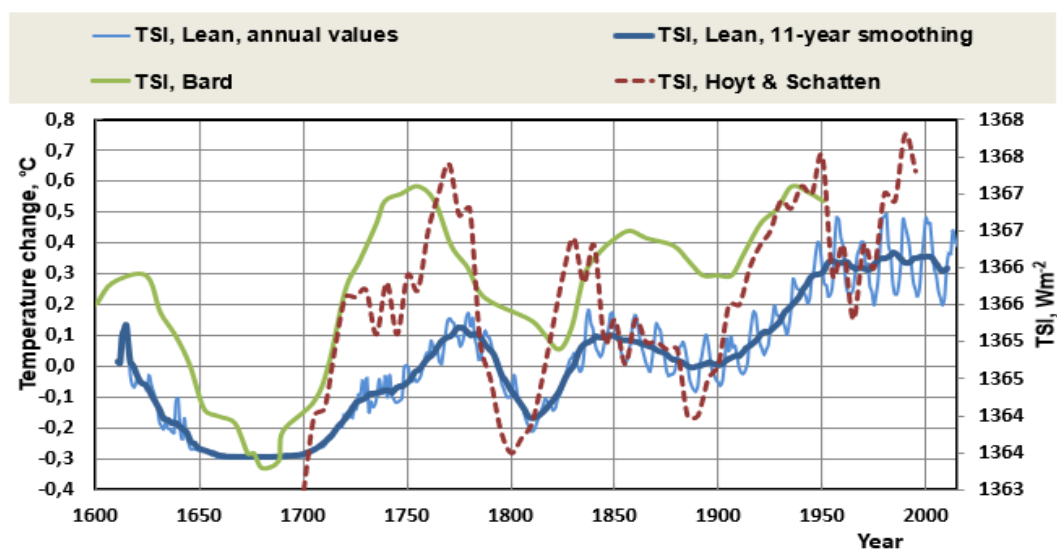


Figure 8. TSI reconstructions of Lean (2004), Hoyt and Schatten (1993), and Bard et al. (1997). The temperature scale applies only to Lean (2004).

According to the data of Lean (2004), the estimated TSI change from 1750 to 2000 has been about 1.1 Wm^{-2} . Based on the latest TSI observations, Lean (2010) has also modified her original TSI estimate of 1366 Wm^{-2} for the 2000s to the modern TSI level of 1361 Wm^{-2} but her estimate for the TSI change is the same 1.1 Wm^{-2} . This TSI change means an RF value of $1.1/4 = 0.275 \text{ Wm}^{-2}$. Connolly et al. (2021) have carried out a comprehensive review study about Sun effects on the Northern Hemisphere temperature trends. Its results show a common feature in all TSI reconstruction studies that around 1900 the TSI value was about -2 Wm^{-2} lower, in the 1930's about $+1 \text{ Wm}^{-2}$ higher, and from 1990 onward about 1.5 Wm^{-2} higher than the reference level. The TSI reconstruction of Velasco Herrera et al. (2015) shows the same general TSI trends as above and they also predict that the TSI trend has a minimum around the 2050s.

A general conclusion can be drawn that the TSI has varied from 1600 onward including low TSI values during the Little Ice Age (LIA, Maunder minimum) and Dalton minimum. The Sun's activity seems to be now at the maximum level starting from 1990 and the TSI value has varied thereafter relatively little according to the Sun's cycle phase of about 11 years (Schwabe cycle).

Kauppinen et al. (2010) and Ollila (2013) have found out from satellite cloudiness observations that a 1 % cloudiness change causes a $0.1 \text{ }^{\circ}\text{C}$ temperature change. Ollila (2017b) has introduced that the TSI impacts cause cloudiness changes and due to this effect, an RF change should be multiplied by a factor of 4.2. By applying this factor, the temperature impact of the TSI change of 1.1 Wm^{-2} from 1750 to 2020 would be $0.32 \text{ }^{\circ}\text{C}$.

3.9 Tree-ring analyses covering the last millennium

Climatic variations leave their mark on the annual rings of trees making it possible to study climate variations. Their thickness growth (tree-ring width) is regulated by the average summer temperature in cool areas and precipitation in arid regions. With the development of dendrochronological methods and the global expansion of research data, the time perspective of research covers the Holocene climate retrospectively. The tree rings are in a special position, as they are the only representative of the year-accurate proxies. In Fig. 9 the results of four tree-ring analyses have been depicted.

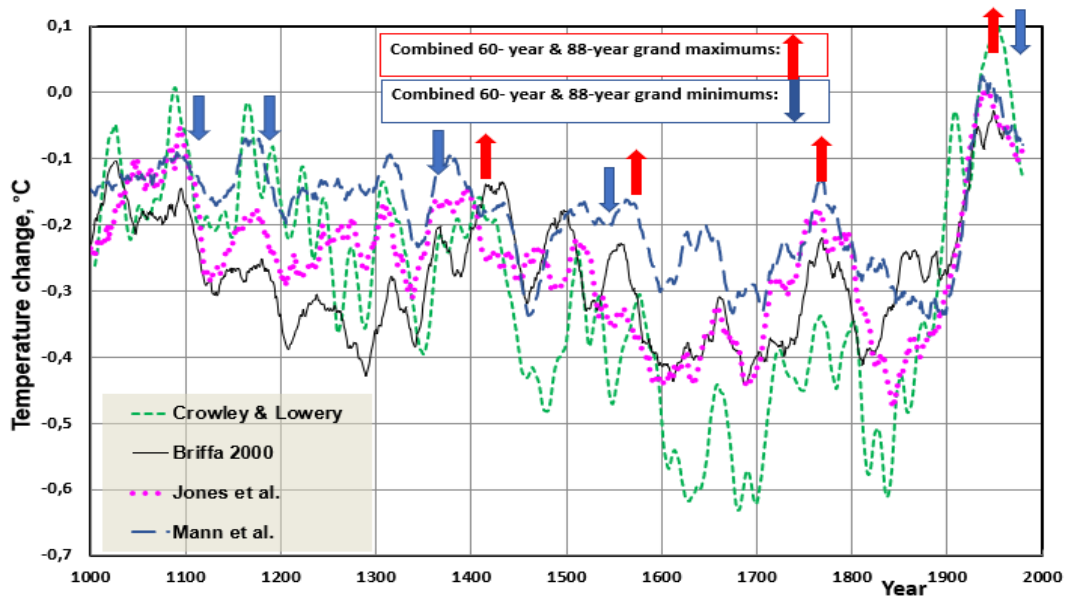


Figure 9. The proxy temperature results of tree-ring analyses of Crowley and Lowery (2000), Briffa (2000), Jones et al. (1998), and Mann et al. (1999). The grand maximums and minimums of 60- and 88-year oscillations have been marked (Ollila and Timonen, 2022).

There are differences in the trends of different tree-ring analyses. Anyway, there is a common tendency that temperatures to start to decline after the beginning of the millennium, there is a minimum during the LIA in the 15th century, and the temperature starts to increase thereafter.

3.10 Summary of temperature proxies of the last millennium

In Fig. 10 three different types of temperature-related proxies have been depicted.

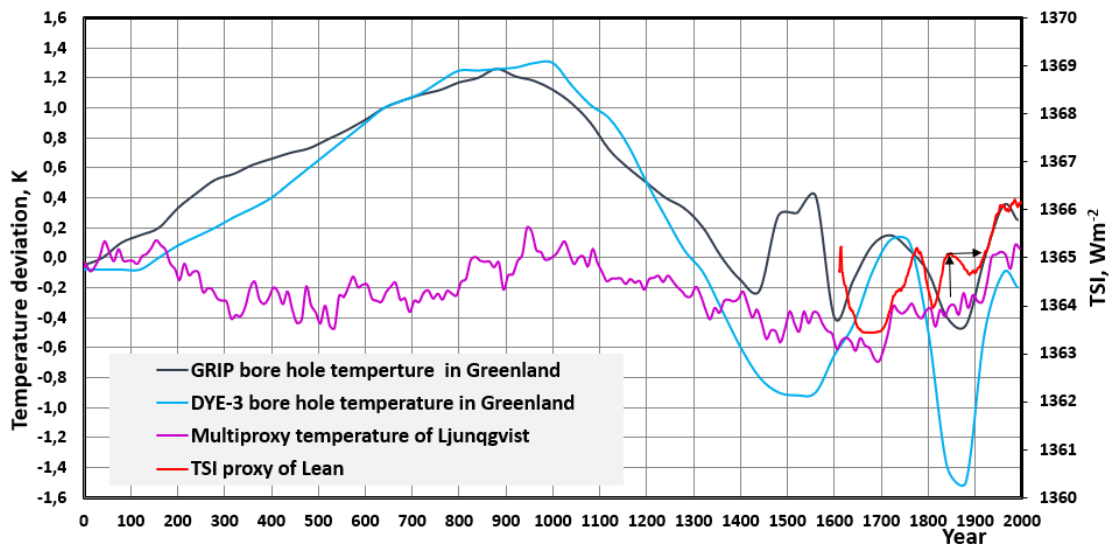


Figure 10. Two proxy temperatures of Greenland's borehole data (Vinther et al, 2011), the multiproxy temperature proxy of Ljungqvist (2010), and the TSI proxy of Lean (1995).

Borehole temperature proxies smooth out short-term variations but they indicate a period of about 1000 years having maximum peaks in about 1000 and the present maximum in 2000 (Hughes et al., 2020; Vinther et al., 2010). The temperature variations seem to be much greater in Greenland than globally, which has also been noticed during the last 50 years.

The temperature data of Ljungqvist (2010) include nine types of temperature data, namely two historical documentary records, three marine sediment records, five lake sediment records, three speleothems $\delta^{18}\text{O}$ records, two ice-core $\delta^{18}\text{O}$ records, four varved thickness sediment records, five tree-ring width records, five tree-ring maximum latewood density records, and one $\delta^{13}\text{C}$ tree-ring record. Because of the combination of different trends, this proxy is rather heavily averaged.

All these proxies show the same kind of temperature trend that during the last millennium, there have been about 1000 yearlong climate oscillations, which is caused by solar activity variations. The Earth is recovering from the LIA and is now at a new maximum.

The IPCC has concluded that the present high temperatures of the 2000s are unprecedented (IPCC, 2013). If the scrutiny period is 2000 years backward, we need not rely on temperature proxy methods only, which show two warm periods (Ljungqvist, 2010) namely the Roman warm period from 250 BC to AD 450 and the Middle Ages warm period from AD 950 to 1250. These well-known warm periods have not happened only in Europe and in North America. Li et al. (2023) have found that during the last 3500 years, the maximum precipitation and temperatures from May to October occurred on the northeastern Tibetan Plateau during the period of 800 – 1400 rather than during the current warm period.

There is also concrete evidence of warmer periods other than temperature proxies. The Lendbreen glacier in Norway is melting and it revealed a well-preserved fabric, which was made according to radiocarbon dating between AD 230 to 390 (Vedeler and Jorgensen, 2013). Retreating Mendenhall glaciers in Alaska has exposed forest remnants growing from 700 to 1000 based on the radiocarbon method according to the statement of Professor Connor (2013). These examples show that these warm periods have been long and at least as warm as the present ones.

3.11 Shortwave radiation anomaly of the 2000s

A significant shortwave (SW) radiation anomaly (later SW_{net}) has been observed by the CERES (2021) satellite measurements from 2001 onward. This trend has been depicted in Fig. 2(a) of Loeb et al. (2021) and in Fig. 7.3 of AR6 (IPCC, 2021). Loeb et al. (2021) concluded that the SW anomaly is probably due to the changes in low-level clouds, and the reasons for these changes may be natural and not known by climate researchers. It should be noted that Marsh and Svensmark (2000) have shown in their study that cosmic rays influence low cloud properties. The SW_{net} , varies according to yearly values of CERES (2021) from 240.36 Wm^{-2} in 2001 to 241.97 Wm^{-2} in 2019, which means an increase of $1,61 \text{ Wm}^{-2}$.

The significant SW anomaly of the 2000s (depicted as shortwave radiation downwelling in Fig. 11) is a reality but its warming impact has not been generally acknowledged in climate science since it challenges the basis of GCMs.

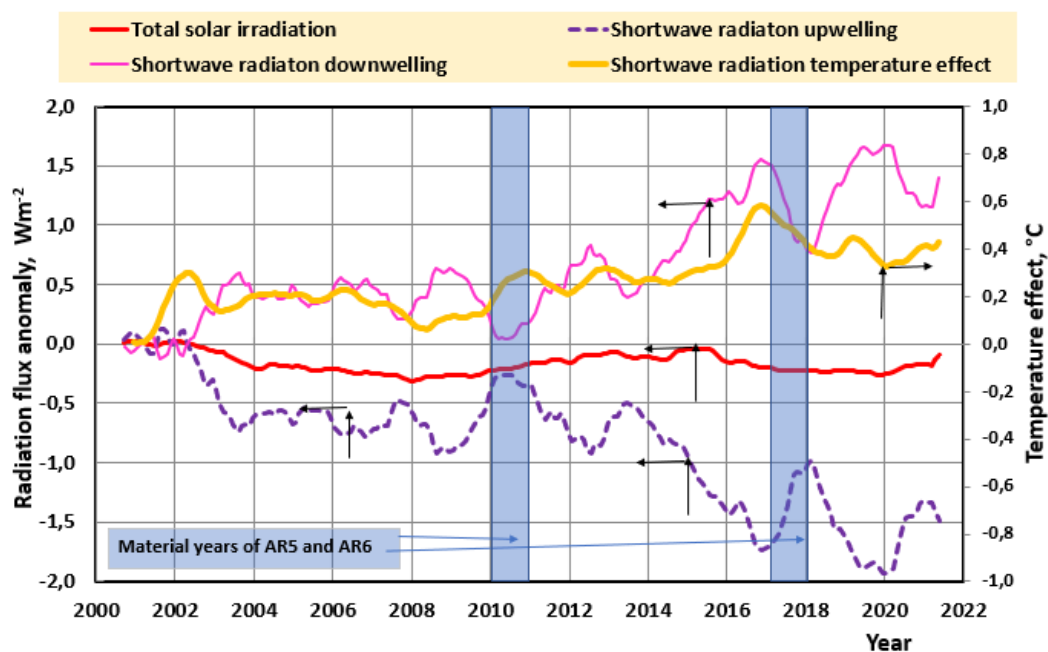


Figure 11. SW and LW radiation changes at the TOA from 2001 to 2020 (Ollila, 2021). The SW_{net} change is the same as the Shortwave radiation downwelling.

The most important issues in climate change are the RF value of CO_2 and the positive water feedback. The SW radiation anomaly of the 2000s created a unique opportunity to test the accuracies of the GCMs applied by the IPCC and a challenging model of Ollila (2021). According to the glossary of AR5 (IPCC, 2013), the portion of any top-of-atmosphere radiative effect that is due to anthropogenic or other external influences, such as changes in the Sun, is termed instantaneous radiative forcing (IRF).

Ollila (2021) simulated the temperature effects during SW radiation anomaly from 2001 to 2019 using both the IPCC's simple climate model and his simple climate model by starting temperature changes from zero in 2001, Fig. 12. In the IPCC model, a λ value of 0.47 Wm^{-2} was applied, and the CO_2 impact was calculated using Eq. (1) and (2), but the other GH gas effects were omitted due to their insignificant impact in the 20-year simulation period. Also, long-term (from 60 to 1000 years) temperature oscillation effects were omitted. For this study, the earlier simulations of the Ollila model were repeated using Eq. (2), with the λ value of 0.265 Wm^{-2} , and the RF value of CO_2 was calculated using Eq. (1). The temperature impact dT of the ENSO effect has been calculated from the Oceanic Nino Index (ONI, 2021), $dT = 0.1 * ONI$ with 6 months delay (Trenberth and Fasullo, 2013; Ollila (2021)). The dynamical time constants for the ocean were 2.74 months, and for land, 1.04 months (Stine et al., 2009).

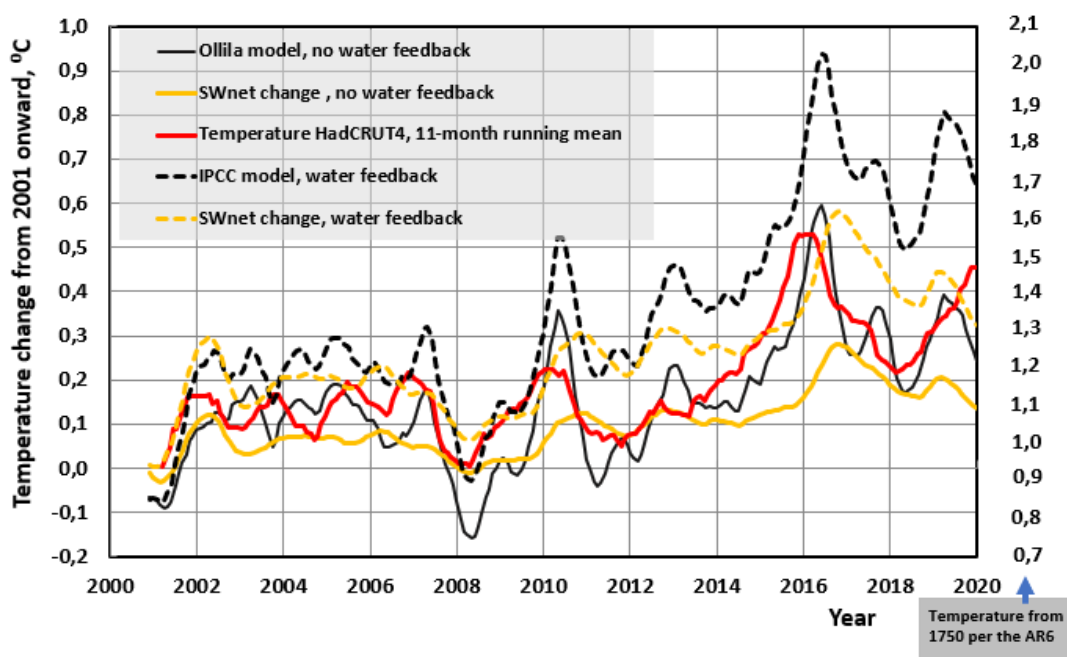


Figure 12. Calculated and observed temperature changes from 2001 to 2020. The SW_{net} changes are the same as in Fig. 11.

The SW_{net} anomaly with the magnitude of 1.75 Wm^{-2} took place under real climate conditions from January 2001 to December 2021; the observed HadCRUT4 (2021) temperature change was $0.46 \text{ }^{\circ}\text{C}$.

The temperature change from 2001 to 2019 according to the IPCC model (Ollila, 2021) is the sum of the SW_{net} change, $0.78 \text{ }^{\circ}\text{C}$, anthropogenic drivers, $0.30 \text{ }^{\circ}\text{C}$, and the ENSO effect, $0.03 \text{ }^{\circ}\text{C}$, to give a total of $1.11 \text{ }^{\circ}\text{C}$, meaning an error of $+0.65 \text{ }^{\circ}\text{C}$ in the HadCRUT4 temperature. The Ollila model (Ollila, 2021) is the sum of a SW_{net} change of $0.40 \text{ }^{\circ}\text{C}$, CO_2 forcing of $0.10 \text{ }^{\circ}\text{C}$, an ENSO effect of $0.03 \text{ }^{\circ}\text{C}$, and cloud effects of $-0.01 \text{ }^{\circ}\text{C}$, for a total of $0.52 \text{ }^{\circ}\text{C}$, meaning an error of $+0.06 \text{ }^{\circ}\text{C}$ in respect of HadCRUT4.

Both model-calculated temperatures follow the ups and downs of the global observations very well indicating that the dynamical time constants are correct. The temperature errors of the IPCC's model are due to the positive water feedback and strong RF value of CO_2 .

It is also interesting to note that during the period from 1979 to 2016, the average error of 102 CMIP5 test runs by Christy (2017) to the observed temperature was $0.55 \text{ }^{\circ}\text{C}$, which is close to the temperature impact of the SW anomaly of $0.43 \text{ }^{\circ}\text{C}$ as calculated by Ollila (2021) from 2001 to 2019 applying simple models.

The IPCC dropped out this change in AR6 model-based temperature calculations since the solar impact has been $-0.01 \text{ }^{\circ}\text{C}$. If the real change according to the IPCC science would have been used, the model-calculated temperature change would have been $1.27 + 0.76 = 2.03 \text{ }^{\circ}\text{C}$ exceeding the Paris agreed temperature limit.

3.12 The summary of anthropogenic and natural drivers

The summary of climate drivers has been summarized in Table 4.

Table 4. The main anthropogenic and natural drivers of surface temperature changes according to IPCC (2013), IPCC (2021), and this study (=NAGW) from 1750 to 2019. The values in parentheses are calculated according to the IPCC science if the SW anomaly of the 2000s is included.

Driver	IPCC/AR5, °C	IPCC/AR6, °C	NAGW, °C
Carbon dioxide	0.84	1.01	0.36
Methane	0.49	0.28	0.14
Nitrogen oxide	0.09	0.10	0.04
Other anthropogenic gases	0.18	0.44	-
Greenhouse gases	1.59	1.83	0.54
Albedo, volcanic	-0.08	-0.09	-
Aerosols, clouds, and contrails	-0.42	-0.49	-
Anthropogenic totally	1.11	1.28	0.54
Solar	0.03	-0.01	0.32
SW radiation anomaly	-	0.00 (0.78)	0.43
Drivers totally	1.17	1.27 (2.03)	1.29
Observed temperature change	0.85°C	1.29°C	1.29°C
Error, %	+37.7%	-1.6% (57%)	0.0%

The most essential result is that according to AR6 (IPCC, 2021), the contribution of CO₂ during the industrial era has been 1.1 °C but according to this study it is 0.36 °C and according to Harde (2022) it is 0.34 °C.

The trend in climate driver magnitudes from AR4 to AR6 is consistent. The most striking feature is the temperature error percentage change from +37.7% in 2011 to -1.6% in 2019 (material years of AR5 and AR6). This change cannot be explained by the abrupt decrease of anthropogenic drivers as noticed in Table 4 figures. A possible reason could be that the surface temperature has paused as it did in the period from 2000 to 2014 but the temperature increase rate has been greater than normal since 2014. The most probable reason is the emerging SW radiation anomaly of 0.43 °C from 2001 to 2019 as indicated in the last column.

3.13 The GH effect and contribution of GH gases

The temperature effect of the GH effect is generally accepted to be 33-34 °C but the radiative force on the Earth's surface causing this temperature increase is getting almost no attention. The cause of the GH effect can be found only in GH effect definitions. The first comprehensive scientific definition of the GH effect based on the present-day knowledge of radiation fluxes and the effects of clouds has been presented by Hartmann (2015): *“Most of this emitted infrared radiation is absorbed by trace gases and clouds in the overlying atmosphere. The atmosphere also emits radiation, primarily at infrared wavelengths, in all directions. Radiation emitted downward from the atmosphere adds to the warming of Earth’s surface by sunlight. This enhanced warming is termed the greenhouse effect.”*

This has not been good enough for the IPCC, which introduced its own definition in the AR5 (2013): *“The longwave radiation (LWR, also referred to as infrared radiation) emitted from the Earth’s surface is largely absorbed by certain atmospheric constituents - (greenhouse gases and clouds) - which themselves emit LWR into all directions. The downward directed component of this LWR adds heat to the lower layers of the atmosphere and to the Earth’s surface (greenhouse effect).”*

They may look very similar, but there is a crucial difference. The AR5 defines that only GH gases

and clouds are responsible for the GH effect. Hartmann does not specify that they are only GH gases and clouds would reradiate downward from the atmosphere, but it is the atmosphere itself, which causes the infrared radiation. So, there might other energy sources which warm up the atmosphere as solar radiation is absorbed by the atmosphere. Hartmann is in line with Planck's law that any material, which has a temperature above absolute zero, will emit electromagnetic radiation according to its temperature.

Ollila (2019) introduced his definition in 2019 and it considers all the energy fluxes warming the atmosphere: *"The Earth's surface emits LW radiation (infrared radiation) and it transfers heat energy in the form of latent and sensible heating into the atmosphere. Most of the emitted infrared radiation is absorbed by trace gases and clouds in the atmosphere. All three energy fluxes increase the temperature of the atmosphere. The part of the infrared radiation due to these three energy sources emitted downward from the atmosphere adds to the warming of Earth's surface by sunlight and it is called the greenhouse effect."*

In AR6 the IPCC (2021) reformulated the GH effect definition and it can be found only in Glossary:

"The infrared radiative effect of all infrared-absorbing constituents in the atmosphere. Greenhouse gases (GHGs), clouds, and some aerosols absorb terrestrial radiation emitted by the Earth's surface and elsewhere in the atmosphere. These substances emit infrared radiation in all directions, but, equal, the net amount emitted to space is normally less than would have been emitted in the absence of these absorbers because of the decline of temperature with altitude in the troposphere and the consequent weakening of emission. An increase in the concentration of GHGs increases the magnitude of this effect; the difference is sometimes called the enhanced greenhouse effect."

This definition does not specify anymore that only the GH gases and clouds are responsible for the downward LW radiation to the Earth's surface like in the AR5 since this radiation has not been noticed at all: only radiation to all directions. It can be speculated that the IPCC noticed its fault in the AR5 definition that the absorption of LW radiation of about 155 Wm^{-2} cannot create the radiation of about 345 Wm^{-2} and tried to fix the problem. This time the IPCC does not show what is causing the GH effect by omitting the downward radiation which is the essence of the GH effect. If you remove the downward radiation, you remove the GH effect.

The existence of the GH effect is a generally acknowledged fact among researchers but the magnitude (the numerical value) of radiative drivers causing the GH effect has not been analyzed in the assessment reports of the IPCC. The GH effect can be illustrated by the energy budget of the Earth, Fig. 13.

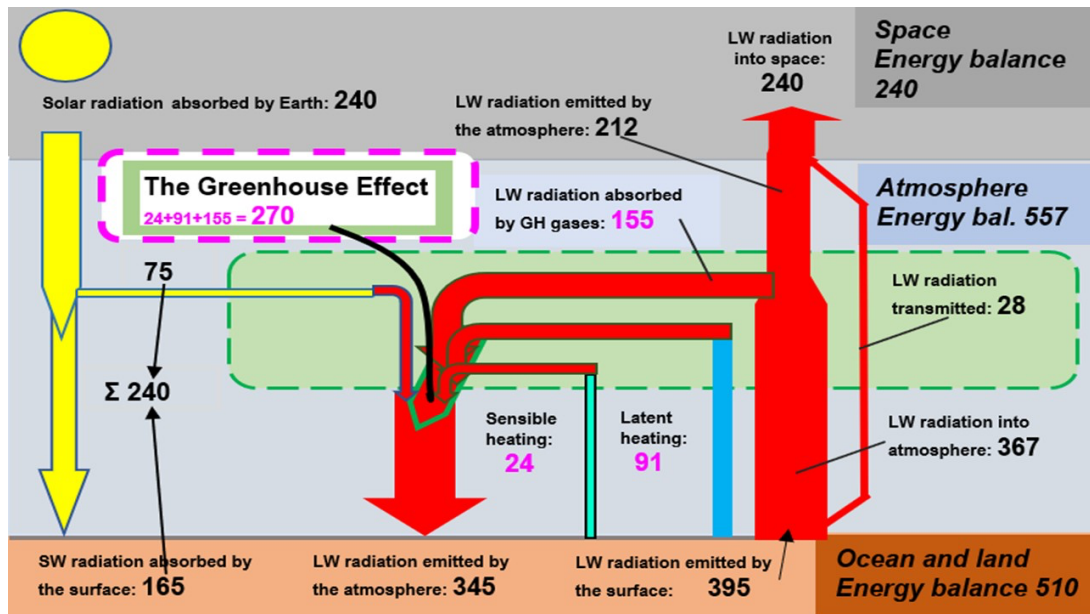


Figure 13. The Earth's energy balance (Ollila, 2019).

The energy balance presented in Fig. 13 is from Ollila (2019). Its numerical flux values are inside the accuracies of Wild et al. (2019), which has been referred to in the AR6 (IPCC, 2021).

The magnitude of the GH effect can be summarized from the flux values in Fig. 13. The reradiation LW flux of 345 Wm^{-2} to the surface is a sum of four fluxes (Wm^{-2}): the absorption of SW radiation 75 , LW absorption by GH gases and clouds 155 , latent heating 91 , and sensible heating 24 . The SW absorption flux of 75 Wm^{-2} together with the SW flux to the surface of 165 Wm^{-2} encompasses the net SW radiation of 240 Wm^{-2} to the Earth. The conclusion is that the GH effect is the sum of three energy fluxes recirculating between the surface and the atmosphere, and its magnitude is 270 Wm^{-2} ($435 - 75 = 270$).

GH effect deniers either say that the downward LW radiation flux of 345 Wm^{-2} is not real or it cannot warm the surface, since it radiates from the atmosphere being colder than the surface. This flux is real and its value can be confirmed by the worldwide measurement network (Driemel et al, 2018). Its reality and meaning are a fact since the energy budget of the surface cannot be closed without this radiation flux. The rate of radiation heat transfer from a body at temperature T_1 which is surrounded by a body at temperature T_2 is given by the Stefan-Boltzmann law

$$Q = \sigma A \epsilon (T_1^4 - T_2^4) [\text{Wm}^{-2}], \quad (7)$$

where σ is the Stefan–Boltzmann constant, A is the surface area of the radiator, and ϵ is the emissivity. The equation means that there is also a heat transfer rate from a colder body since all material radiates electromagnetic radiation according to Planck's law. The surface temperature T_1 is a result of these two heat transfer rates. The observation based on average radiation flux values over the period 1985-1988 shows that in the clear-sky conditions, the LW radiation upward is 394.1 Wm^{-2} and downward 313.5 Wm^{-2} but in the cloudy-sky conditions LW radiation upward is 396.3 Wm^{-2} , and downward 359.0 Wm^{-2} . These figures mean that during relatively short periods of a few days (about two days of three are cloudy), the surface temperature is higher in cloudy-sky conditions even though the SW radiation to the surface decreases by 68.3 Wm^{-2} . This would not be possible without the simultaneous increase of LW radiation by 45.5 Wm^{-2} .

Practical examples of the warming effect of different sky conditions and the S-B law are carports used in Scandinavian countries: the car windows below open car roofs stay clear in temperatures

from -0 °C to -25 °C when adjacent car windows under the open sky become frozen.

LW radiation excluding the SW radiation absorption radiation is the basis for calculating the contributions of GH gases and clouds to the GH effect. The most referred figure (Kiehl and Trenberth, 2009) of the CO₂ contribution is 26 %. Climate change researchers should realize that this result is calculated in the modified US Standard Atmosphere 76 (US 76) containing 50 % less water than the average global atmosphere (Ollila, 2014). The US 76 has also been called “a standard atmosphere”, creating a wrong image (Liou, 1992).

Schmidt et al. (2010) have used the average atmospheric composition and the GH effect magnitude of 155 Wm⁻² in calculating the contributions of GH gases and clouds in the GH effect. Their results and the same of Ollila (2017a) have been summarized in Table 5.

Table 5. The contributions of GH gases and clouds in the GH effect according to Kiehl & Trenberth (1997), Michell (1989), Schmidt et al. (2010), and Ollila (2017a).

GH effect element	Ollila		Kiehl & Trenberth	Michell	Schmidt et al.
LW absorption element	RF, Wm ⁻²	Contr., %	Contr., %	Contr., %	Contr., %
Water	90.9	33.6	60 (38)	65	50
Carbon dioxide	20.1	7.4	26	32	19
Ozone	6.9	2.6	8	1	
Methane & Nitrogen oxide	1.8	0.7	6	2	7
Clouds	35.9	13.3	(39)		25
<i>LW absorption</i>	<i>155.6</i>		<i>125 (155)</i>		<i>155</i>
Latent heating	90.8	33.6			-
Sensible heating	24.2	8.9			-
GH effect	270.6		155		155

Michell (1989) has not specified the atmosphere. The %-values in parentheses of Kiehl & Trenberth are for cloudy sky conditions. The major reason for a much lower contribution-% of CO₂ by Ollila (2017a) is the magnitude of the GH effect 270.6 Wm⁻² versus the 155 Wm⁻² of Schmidt et al. (2010); the absorption value of CO₂ is practically the same in both papers. A counterargument against the calculation basis of 270 Wm⁻² could be that latent heating does not change the surface temperature, and the difference between the surface emitted radiation 395 Wm⁻² and the net radiative flux from the Sun is 395 – 240 = 155 Wm⁻², which is exactly the absorption magnitude by GH gases and clouds.

The reradiation of 345 Wm⁻² is the sum of all four energy fluxes warming the atmosphere. This radiation flux warms up evenly the surface and it has an even-handed contribution to three energy fluxes cooling the surface: the LW radiation, latent and sensible heating. We cannot conclude that the latent heating energy originates only from the latent heating part of atmospheric reradiation. In the same way, we cannot conclude that the SW absorption flux of 75 Wm⁻² contributes only to the radiation capability of the surface, but it does not contribute the latent and sensible heating. Every component warming up the atmosphere contributes to the GH effect (LW reradiation minus SW absorption) according to its energy flux absorbed in the atmosphere. The situation in the climate zones shows that latent and sensible heating is related to the high temperatures of the tropical zone. Therefore, the real GH effect is the sum of LW absorption in the atmosphere, latent heating, and sensible heating.

5. Conclusions and discussion

The alternative climate model NAGW including natural and anthropogenic drivers can explain the long-term global warming from 1750 onward as well the short-term warming during the 2000s.

The summary of the differences between the most important key figures of the IPCC and the challenging NAGW is tabulated in Table 3. The known TSI variations have an important role in explaining the warming before 1880. There are two warming periods since 1930 and the cycling AHR effects can explain these periods of 60-year intervals. The warming mechanisms of TSI and AHR include cloudiness changes and these quantitative effects are based on empirical temperature changes. This review concludes that the NAGW has a solid theoretical background, and its warming value has better conformity with the observed temperature than the AGW. The major parameters of the AR6 (IPCC, 2021) and the parameters applied in the NAGW are collected in Table 6.

Table 6. The summary of differences between the IPCC (2021) and this study including uncertainty limits.

Parameter	AR6, IPCC	NAGW
CO ₂ contribution to the GH effect	About 19 % – 26 %	7 % – 8 %
H ₂ O contribution in the GH effect	About 50 % – 69 %	66 % – 69 %
Water feedback	Amplifies GH gas effects by a factor from 2 to 3	Only short-term (1-2 years) positive feedback
Climate sensitivity parameter (λ)	0.47 K/(Wm ⁻²) ± 0.03	0.265 K/(Wm ⁻²) ± 0.05
RF value of 2 * CO ₂	3.93 Wm ⁻² ± 0.47 Wm ⁻²	2.4 Wm ⁻² ± 0.3 Wm ⁻²
Anthrop. CO ₂ in the atmosphere in 2019	265 GtC	70 GtC
The residence time of anthropogenic CO ₂	From centuries to millennia	16 years ± 1 years
The residence time of total CO ₂	Same as anthropogenic CO ₂	70 years ± 10 years
Transient Climate Response – TCR	1.8 °C (1.4 °C + 2.2 °C)	0.6 °C ± 0.15°C
Equilibrium climate sensitivity - ECS	3.0 °C (2.5 °C – 4.0 °C)	0.6 °C ± 0.15 °C
Greenhouse effect	159 Wm ⁻²	270 Wm ⁻²

The differences and the reason for them are already analyzed in the former sections. The most important differences are the water feedback and the RF formula of CO₂. These two differences explain the differences in CS values. Considering the future atmospheric CO₂ concentration development, also the residence time difference is very essential. Table 6 does not show the temperature effect of the SW radiation anomaly, which is not included in GCM simulations in the AR6 calculations for 2019, and which is about 0.78 °C.

Because the Sun's activity should be decreasing and the AHR effect also declines after a few years, the global temperature according to this alternative warming theory should decline permanently after 2020 even though the warming effect of GH gases increases steadily.

Conflicts of interest/competing interests: The author has no conflicts of interest to declare that are relevant to the content of this article.

Funding: No funding was received for conducting this study.

Guest-Editor: Stein Storlie Bergsmark; Reviewers: anonymous.

References

- Agnihotri R, Dutta K, Bhushan R, Somayajulu BLK, 2002: Evidence for solar forcing on the Indian monsoon during the last millennium. *Earth and Planet Sci Lett*, 198, 521-527. [https://doi.org/10.1016/S0012-821X\(02\)00530-7](https://doi.org/10.1016/S0012-821X(02)00530-7)
- Attolini MR, Cecchini S, Galli M, Nanni T, 1987: The Gleissberg and 130-year periodicity in the cosmogenic isotopes in the past: The Sun as a quasi-periodic system. *Proceedings of the 20th International Cosmic Ray Conference, Moscow*, 4, 323, Nauka, Moscow. <https://articles.adsabs.harvard.edu/pdf/1987ICRC...20d.323A>
- Bard E, Raisbeck G, Françoise You F, Jouzel J, 1997: *Solar modulation of cosmogenic nuclide production over the last millennium: comparison between ¹⁴C and ¹⁰Be records*. *Earth & Planet Sci Lett*, 150, 0–462. [https://doi.org/10.1016/S0012-821X\(97\)00082-4](https://doi.org/10.1016/S0012-821X(97)00082-4)
- Bard E, Raisbeck G, Françoise You F, Jouzel J, 2000: *Solar irradiance during the last 1200 years based on cosmogenic nuclides*. *Tellus*, 52B, 985–992. <https://doi.org/10.1034/j.1600-0889.2000.d01-7.x>
- Barrett J, Bellamy D, Hug H, 2006: *On the sensitivity of the atmosphere to the doubling of the carbon dioxide concentration and on water vapour feedback*. *E&E*, 17(4), 603-607. <https://sci-hub.wf/10.1260/095830506778644198>
- Bengtsson L, Schwartz SE, 2013: *Determination of a lower bound on Earth's climate sensitivity*. *Tellus B Chem Phys Meteorol*, 65:1. DOI: [10.3402/tellusb.v65i0.21533](https://doi.org/10.3402/tellusb.v65i0.21533)
- Berry EX, 2021: *The impact of human CO₂ of atmospheric CO₂*. *Sci Clim Change*, 1.2, 213-249. <https://scienceofclimatechange.org/wp-content/uploads/Berry-2021-Impact-of-human-CO2.pdf>
- Briffa KR, Osborn TJ, Schweingruber FH, Harris IC, Jones PD, Shiyatov SG, Vaganov EA, 2001: *Low-frequency temperature variations from a northern tree ring density network*. *J Geophys Res Atmos*, 106, 2929–2941. <https://doi.org/10.1029/2000JD900617>
- Bond G, 1997: *A Pervasive Millennial-Scale Cycle in North Atlantic Holocene and Glacial Climates*. *Science*, 278(5341), 1257–1266. DOI: [10.1126/science.278.5341.1257](https://doi.org/10.1126/science.278.5341.1257)
- CERES, 2021: The National Oceanic and Atmospheric Administration (NOAA), *CERES EBAF-TOA Data*: <https://ceres-tool.larc.nasa.gov/ord-tool/jsp/EBAFTOA41Selection.jsp>
- Chen D, Wang H, Sun J, Gao Ya, 2018: *Pacific multi-decadal oscillation modulates the effect of Arctic oscillation and El Niño southern oscillation on the East Asian winter monsoon*. *Int J Clim*, 38, 2808-2818. <https://doi.org/10.1002/joc.5461>
- Christy JA, 2017: *Testimony*. U.S. House Committee on Science, Space & Technology. <https://docs.house.gov/pdf>

Cini Castagnoli G, Bonino G, Serio M, Sonett CP, 1992: *Common spectral features in the 5500-year record of total carbonate in sea sediments and radiocarbon in tree rings*. Radiocarbon, 34(3), 798–805. DOI: <https://doi.org/10.1017/S0033822200064109>

Connolly R, Soon W, Connolly M, Baliunas S, Berglund, 2021: *How much has the Sun influenced Northern Hemisphere temperature trends? An ongoing debate*. Res Astron Astrophys, 21, 31. <https://iopscience.iop.org/article/10.1088/1674-4527/21/6/131/meta>

Connor C, 2013: *Statement of Professor Connor*. Ancient forest thaws from melting glacial tomb. <https://www.livescience.com/39819-ancient-forest-thaws.html>

Crowley TJ, Lowery TS, 2000: *How Warm Was the Medieval Warm Period?* J Hum Environ Stud, 29(1), 51–54. <https://doi.org/10.1579/0044-7447-29.1.51>

Dansgaard W, Johnsen SJ, Clausen HB, Dahl-Jensen D, Gundestrup N, Hammer CU, Oeschger H, 1984: *North Atlantic climatic oscillations revealed by deep Greenland ice cores*. Geophys Monogr Ser Climate Processes and Climate Sensitivity 29, 288–298. <https://doi.org/10.1029/GM029p0288>

Dansgaard W, Johnsen SJ, Clausen HB, Dahl-Jensen D, Gundestrup NS, Hammer CU, Hvidberg CS, Steffensen JP, Sveinbjörnsdóttir AE, Jouzel J, 1993: *Evidence for general instability of past climate from a 250-kyr ice-core record*. Nature, 364(6434), 218–220. <https://doi.org/10.1038/364218a0>

Davis WJ, 2017: *The relationship between atmospheric carbon dioxide concentration and global temperature for the last 425 million years*. Climate 5(4), 76. <https://doi.org/10.3390/cli5040076>

Davis W, Taylor P, Davis W, 2018: *The Antarctic centennial oscillation: A natural paleoclimate cycle in the southern hemisphere that influences global temperature*. Climate, 6(1), 3. <https://doi.org/10.3390/cli6010003>

Davis WJ, Taylor PJ, Davis WB, 2019: *The origin and propagation of the Antarctic centennial oscillation*. Climate, 7(9), 112. <https://doi.org/10.3390/cli7090112>

Driemel A, Augustine J, Behrens K, Colle S, Cox C, et. 2018: *Baseline Surface Radiation Network (BSRN): structure and data description (1992–2017)*. Earth Sys Sci Data, 10(3), 1491–1501. <https://doi.org/10.5194/essd-10-1491-2018>

Drotos G, Becker T, Mauritsen T, Stevens B, 2020: *Global variability in radiative-convective equilibrium with a slab ocean under a wide range of CO₂ concentrations*. Tellus A: Dyn Meteorol Oceanogr, 72(1), 1–1. <https://sci-hub.wf/10.1080/16000870.2019.1699387>

Ermakov VJ, Okhlopkov VP, Stozhkov YuI, 2009: *Influence of cosmic rays and cosmic dust on the atmosphere and Earth's climate*. Bull Russ Acad Sci: Phys, 73, 434–436. <https://doi.org/10.3103/S1062873809030411>

Etminan E, Myhre G, Highwood EJ, Shine KP, 2016: *Radiative forcing of carbon dioxide, methane, and nitrous oxide: A significant revision of methane radiative forcing*. Geophys Res Lett 43:12614-12636. <https://doi.org/10.1002/2016GL071930>

Feynman J, Fougere PF, 1984: *Eighty-eight-year periodicity in solar-terrestrial phenomena confirmed*. J Geophys Res: Space Phys, 89, 3023–3027. <https://doi.org/10.1029/JA089iA05p03023>

Fleming RJ, 2018: *An updated review about carbon dioxide and climate change*. Environ Earth Sci, 77(6), 262–. <https://link.springer.com/article/10.1007/s12665-018-7438-y>

Folland CK, Parker DE, Kates FE, 1984: *Worldwide marine temperature fluctuations 1856–1981*. Nature, 310, 670–673. <https://doi.org/10.1038/310670a0>

Folland CK, Parker DE, Kates FE, 1986: *Sahel rainfall and worldwide sea temperatures, 1901-85*. Nature, 320, 602-607. <https://doi.org/10.1038/320602a0>

Friedlingstein P, Jones MW, O'Sullivan M, Robbie MA, Hauck J, et al., 2020: *Global Carbon Budget 2020*. Earth Syst Sci Data 12:3269-3340. <https://doi.org/10.5194/essd-12-3269-2020>

Gats, 2014: *Spectral calculations tool*, <http://www.spectralcalc.com/info/about.php>

Gervais F, 2021: *Climate sensitivity and carbon footprint*. Sc Clim Change, 1.1, 70-97. <https://scienceofclimatechange.org/wp-content/uploads/Gervais-2021-Climate-Sensitivity-Carbon-Footprints.pdf>

Gruber N, Clement D, Carter B, Feely RA, van Heuven S, Hoppema M, Ishii M, Key RM, Kozyr A, Lauvset SK, Lo Monaco C, Mathis JT, Murata A, Olsen A, Perez FF, Sabine, CL, Tanhua T, Wanninkhof R, 2019: *The oceanic sink for anthropogenic CO₂ from 1994 to 2007*. Science, 363(6432), 1193–1199. doi: [10.1126/science.aau5153](https://doi.org/10.1126/science.aau5153)

Hale GE, 1908: *On the probable existence of a magnetic field in sunspots*. Astrophys J, 28, 315-343. [10.1086/141602](https://doi.org/10.1086/141602)

HadCRUT4, 2021: *HadCRUT4 temperature data of Met Office Hadley Centre*. <https://www.met-office.gov.uk/hadobs/hadcrut4/>

Harde H, 2013: *Radiation and heat transfer in the atmosphere: A comprehensive approach on a molecular basis*. Int J Atmos Sci, ID 503727. <https://doi.org/10.1155/2013/503727>

Harde H, 2017: *Radiation transfer calculations and assessment of global warming by CO₂*. Int J Atmos Sci, <https://downloads.hindawi.com/archive/2017/9251034.pdf>

Harde H, 2022: *How Much CO₂ and the Sun Contribute to Global Warming: Comparison of Simulated Temperature Trends with Last Century Observations*. Sc Clim Change, 2.2, 105-133. <https://scienceofclimatechange.org/wp-content/uploads/Harde-2022-CO2-Sun-Global-Warming.pdf>

- Harde H, Salby ML, 2021: What Controls the Atmospheric CO₂ Level? *Sci Clim Change*, 1.1, 54-69. <https://scienceofclimatechange.org/wp-content/uploads/Harde-and-Salby-2021-What-Controls-CO2.pdf>
- Hartmann DL, 2015: *Global Physical Climatology*, Elsevier Science, USA. <https://www.elsevier.com/books/global-physical-climatology/hartmann>
- Hauck J, Zeising M, Le Quéré C, Gruber N, Bakker DCE, Bopp L, et al., 2020: *Consistency and challenges in the ocean carbon sink estimate for the global carbon budget*. *Front Mar Sci*, 7, 852. <https://doi.org/10.3389/fmars.2020.571720>
- HITRAN, 2021: *High-Resolution Transmission Molecular Absorption data base*, Harvard-Smithsonian Center for Astrophysics. <https://www.cfa.harvard.edu/hitran/>
- Hoyt DV, Schatten KH, 1993: *A discussion of plausible solar irradiance variations, 1700-1992*. *J Geophys Res*, 98(A11), 18895-18906. <https://doi.org/10.1029/93JA01944>
- Hughes AG, Jones TR, Vinther BM, Gkinis V, Stevens CM, Morris V, Vaughn BH, Holme C, Markle BR, Whiter JWC, 2020: *High-frequency climate variability in the Holocene from a coastal-dome ice core in east-central Greenland*. *Clim Past*, 16, 1369–1386. <https://doi.org/10.5194/cp-16-1369-2020>
- Humlum O, Stordahl K, Solheim J-E, 2013: *The phase relation between atmospheric carbon dioxide and global temperature*. *Glob Planet Change*, 100, 51–69. <https://www.sciencedirect.com/science/article/abs/pii/S0921818112001658?via%3Dihub>
- Jones PD, Briffa KR, Barnett TP, Tett SFB, 1998: *High-resolution paleoclimatic records for the last millennium: interpretation, integration, and comparison with General Circulation Model control-run temperatures*. *Holocene*, 8(4), 455–471. <https://doi.org/10.1191/095968398667194956>
- IPCC, 2001: *Climate Change 2001, The Physical Science Basis, TAR*, (eds. Salomon S. et al.). Cambridge Univ. Press, UK. https://www.ipcc.ch/site/assets/uploads/2018/03/WGI_TAR_full_report.pdf
- IPCC, 2007: *Climate Change 2007, The Physical Science Basis, AR4*, (eds. Salomon S. et al.). Cambridge Univ. Press, UK. <https://www.ipcc.ch/report/ar4/wg1/>
- IPCC, 2013: *Climate Change 2011, The Physical Science Basis, AR5*, (eds. Salomon S. et al.). Cambridge Univ. Press, UK. https://www.ipcc.ch/site/assets/uploads/2017/09/WG1AR5_Front-matter_FINAL.pdf
- IPCC, 2021: *Climate Change 2021, The Physical Science Basis, AR6*, Cambridge Univ. Press, UK. <https://www.ipcc.ch/report/ar6/wg1/>
- Joos F, Prentice IC, Sitch S, Meyer R, Hooss G, et al., 2001: *Global warming feedbacks on terrestrial carbon uptake under the Intergovernmental Panel on Climate Change (IPCC) Emission Scenarios*, *Glob Biogeochem Cycles*, 15, J891-908. [10.1029/2000GB001375](https://doi.org/10.1029/2000GB001375)

- Joos F, Roth R, Fuglestedt JS, Peters GP, Enting IG, 2013: *Carbon dioxide and climate impulse response functions for the computation of greenhouse gas metrics: a multi-model analysis*. *Atm Chem Phys*, 13(5): 2793–2825. [doi:10.5194/acp-13-2793-2013](https://doi.org/10.5194/acp-13-2793-2013)
- Kauppinen J, Heinonen JT, Malmi PJ, 2014: *Influence of relative humidity and clouds on the global mean surface temperature*. *E&E* 25(2). <https://doi.org/10.1260/0958-305X.25.2.389>
- Kerr RA, 2000: *A North Atlantic Climate Pacemaker for the Centuries*. *Science*, 288,1984-1985. DOI: [10.1126/science.288.5473.1984](https://doi.org/10.1126/science.288.5473.1984)
- Kiehl JT, Trenberth KE, 1997: *Earth's annual global mean energy budget*. *Bull Amer Meteor Soc* 90: 311-323. [https://doi.org/10.1175/1520-0477\(1997\)078<0197:EAGMEB>2.0.CO;2](https://doi.org/10.1175/1520-0477(1997)078<0197:EAGMEB>2.0.CO;2)
- Kissin YV, 2015: *A simple alternative model for the estimation of the carbon dioxide effect on the Earth's energy balance*. *E&E*, 26(8), 1319–1333. <https://doi.org/10.1260/0958-305X.26.8.1319>
- Klyashtorin LB, Borisov V, Lyubushin A, 2009: *Cyclic changes of climate and major commercial stocks of the Barents Sea*. *Mar Biol Res*, 5, 4-17. <https://doi.org/10.1080/17451000802512283>
- Lean J, 1995: *Construction of solar irradiance since 1610: Implications for climate change*. *Geophys Res Lett* 22: 3195-3198. <https://doi.org/10.1029/95GL03093>
- Lean J, 2004: *Solar Irradiance Reconstruction*, IGBP PAGES/World Data Center for Paleoclimatology Data Contribution Series # 2004-035, NOAA/NGDC Paleoclimatology Program.
- Lean J, 2010: *Cycles and trends in solar irradiance*. *WIREs Climate Change* 1: 111-122. <https://doi.org/10.1002/wcc.18>
- Levin I, Naegler T, Kromer B, Diehl M, Francey RJ, Gomez-Pelaez AJ, Steele LP, Wagenbach D, Weller R and Worthy DE, 2010: *Observations and modelling of the global distribution and long-term trend of atmospheric ¹⁴CO₂*. *Tellus* 62B, 26-46. DOI: [10.1111/j.1600-0889.2009.00446.x](https://doi.org/10.1111/j.1600-0889.2009.00446.x)
- Lewis N, Curry JA, 2015: *The implications for climate sensitivity of AR5 forcing and heat uptake estimates*. *Clim Dyn*, 45(3-4), 1009–1023. <https://doi.org/10.1007/s00382-014-2342-y>
- Li Y, Wu D, Wang T, Chen L, Chenbin Z, 2023: *Late Holocene temperature and precipitation variations in an alpine region of the northeastern Tibetan Plateau and their response to global climate change*. *Palaeogeogr Palaeoclimatol Palaeoecol* 615(3), 111442. <https://doi.org/10.1016/j.palaeo.2023.111442>
- Lin YC, Fan CY, Damon PE, Wallick EI, 1975: *Long-term modulation of cosmic-ray intensity and solar activity cycles*, 14th International Cosmic Ray Conference, Germany, Munchen, 3, 995–999. Max-Planck-Institut für extraterrestrische Physik, Germany. <https://adsabs.harvard.edu/full/1975ICRC....3..995L>
- Liou KN, 1992: *Radiation and cloud processes in the atmosphere*. Oxford Univ. Press, UK. <https://www.osti.gov/biblio/7081459>

LLNL, 2016: Lawrence Livermore National Laboratory, ¹⁴C “Bomb Pulse” Pulse Forensics, <https://cams.llnl.gov/cams-competencies/forensics/14c-bomb-pulse-forensics>

Locean, 2016: *Oceans 13C*, <https://www.locean-ipsl.upmc.fr/oceans13c/indexAng.htm>

Loeb NG, Johnson GC, Thorsen TJ, Lyman JM, Rose FG, Kato S, 2021: *Satellite and ocean data reveal marked increase in Earth’s heating rate*. *Geophys Res Lett*, 48, e2021GL093047. <https://doi.org/10.1029/2021GL093047>

Loehle C, 2014: *The epistemological status of general circulation models*. *Ecol Modell*, 276(), 80–84. <https://doi.org/10.1007/s00382-017-3717-7>

Lungqvist FC, 2010: *A new reconstruction of temperature variability in the extra-tropical Northern Hemisphere during the last two millennia*. *Geogr Ann*, 92 A 3, 339–351. <https://doi.org/10.1111/j.1468-0459.2010.00399.x>

Manabe S, Wetherald R, 1967: *Thermal equilibrium of the atmosphere with a given distribution of relative humidity*. *J Atmos Sci* 24, 241–259. [https://doi.org/10.1175/1520-0469\(1967\)024<0241:TEOTAW>2.0.CO;2](https://doi.org/10.1175/1520-0469(1967)024<0241:TEOTAW>2.0.CO;2)

Mann ME, Bradley RS, Hughes MK, 1999: *Northern hemisphere temperatures during the past millennium: Inferences, uncertainties, and limitations*. *Geophys Res Lett*, 26(6), 759–762. <https://doi.org/10.1029/1999GL900070>

Marsh ND, Svensmark H, 2000: *Low cloud properties influenced by cosmic rays*. *Phys Rev Lett*, 85, 5004–5007. <https://doi.org/10.1103/PhysRevLett.85.5004>

Meinshausen M, Nicholls MRJ, Lewis J, Gidden MJ, Vogel E, et al., 2020: *The shared socio-economic pathway (SSP) greenhouse gas concentrations and their extensions to 2500*. *Geosci Model Dev* 13, 3571–3605. <https://doi.org/10.5194/gmd-13-3571-2020>

Michell JFB, 1989: *The “greenhouse” effect and climate change*. *Rev Geophys*, 27(1), 115–139. <https://doi.org/10.1029/RG027i001p00115>

Miskolczi FM, Mlynczak MG, 2004: *The greenhouse effect and the spectral decomposition of the clear-sky terrestrial radiation*. *Időjaras* 108, 209–251. http://owww.met.hu/idojaras/IDOJA-RAS_vol108_No4_01.pdf

Miskolczi FM, 2014: *The greenhouse effect and the infrared radiative structure of the Earth's atmosphere*. *Dev Earth Sc* 2, the greenhouse effect. https://www.researchgate.net/publication/268507883_The_Greenhouse_Effect_and_the_Infrared_Radiative_Structure_of_the_Earth's_Atmosphere

Myhre G, Highwood EJ, Shine KP, Stordal F, 1998: *New estimates of radiative forcing due to well mixed greenhouse gases*. *Geophys. Res. Lett.* 25, 2715–2718. <https://doi.org/10.1029/98GL01908>

Myhre G, Stordal F, Gausemel I, Nielsen CJ, Mathieu E, 2016: *Line-by-line calculation of thermal infrared radiation for global condition: CFC-12 as an example*. *J Quant Spectros Radiat Transf* 97, 317–331. <https://doi.org/10.1016/j.jqsrt.2005.04.015>

NOAA, 2021: NCEP/NCAR Reanalysis Data. <https://www.esrl.noaa.gov/psd/cgi-bin/data/timeseries/timeseries1.pl>

NOAA, 2018: *The data: What ¹³C tells us, the global view 2018*. <http://www.esrl.noaa.gov/gmd/outreach/isotopes/c13tellsus.html>.

NOAA, 2022: *Atlantic Multidecadal Oscillation AMO (2022)*. <https://psl.noaa.gov/data/correlation/amon.us.long.data>

NSDC, 2020: Six tree-ring proxy data and one temperature data set. https://www1.ncdc.noaa.gov/pub/data/paleo/tree-ring/reconstructions/n_hem_temp/briffa2001jgr3.txt

Ohmura A, 2013: *Physical basis for the temperature-based melt-index method*. J Appl Meteorol 40, 753-761. [https://doi.org/10.1175/1520-0450\(2001\)040<0753:PBFTTB>2.0.CO;2](https://doi.org/10.1175/1520-0450(2001)040<0753:PBFTTB>2.0.CO;2)

ONI, 2021: *Oceanic Nino Index (ONI) of NOAA*: <https://ggweather.com/enso/oni.htm>

Ollila A, 2012: *The roles of greenhouse gases in global warming*. Energy Environ, 23(5), 781-799. <https://doi.org/10.1260/0958-305X.23.5.781>

Ollila A, 2013: *Dynamics between clear, cloudy and all-sky conditions: cloud forcing effects*. J Chem Biol Phys Sc 4(1), 557-575. https://www.researchgate.net/publication/274958251_Dynamics_between_clear_cloudy_and_all-sky_conditions_Cloud_forcing_effects

Ollila A, 2014: Dev Earth Sci 2, 20-30 *The potency of carbon dioxide (CO₂) as a greenhouse gas*. https://www.researchgate.net/publication/274956207_The_potency_of_carbon_dioxide_CO2_as_a_greenhouse_gas

Ollila A, 2017a: *Warming effect reanalysis of greenhouse gases and clouds*. Phys Sci Int J 13(2), 1-13. DOI: 10.9734/PSIJ/2017/30781. [DOI: 10.9734/PSIJ/2017/30781](https://doi.org/10.9734/PSIJ/2017/30781)

Ollila A, 2017b: *Semi empirical model of global warming including cosmic forces, greenhouse gases, and volcanic eruptions*. Phy Sci Int J 15(2), 1-14. [DOI:10.9734/PSIJ/2017/34187](https://doi.org/10.9734/PSIJ/2017/34187)

Ollila A, 2019: *The greenhouse effect definition*. Phy Sci Int J 23(2), 1-5. [DOI: 10.9734/PSIJ/2019/v23i230149](https://doi.org/10.9734/PSIJ/2019/v23i230149)

Ollila A, 2020a: *The pause end and major temperature impacts during super El Niños are due to shortwave radiation anomalies*. Phys Sc Int J 24(2):1-20. [DOI: 10.9734/PSIJ/2020/v24i230174](https://doi.org/10.9734/PSIJ/2020/v24i230174)

Ollila A, 2020b: *The Greenhouse effect calculations by an iteration method and the issue of stratospheric cooling*. Phy Sci Int J 24(7), 1-18. [DOI: 10.9734/PSIJ/2020/v24i730199](https://doi.org/10.9734/PSIJ/2020/v24i730199)

Ollila A, 2020c: *Analysis of the simulation results of three carbon dioxide (CO₂) cycle models*. Phys Sc Int J 23(4),1-19. [DOI: 10.9734/PSIJ/2019/v23i430168](https://doi.org/10.9734/PSIJ/2019/v23i430168)

Ollila A, 2021: *Global Circulations Models (GCMs) simulate the current temperature only if the shortwave radiation anomaly of 2000s has been omitted*. Phys Sc Int J 40(17), 45-52. [DOI:10.9734/CJAST/2021/v40i1731433](https://doi.org/10.9734/CJAST/2021/v40i1731433)

- Ollila A, Timonen M, 2022a: *Two main temperature periodicities related to planetary and solar activity oscillations*. Int J Clim, <https://doi.org/10.1002/joc.7912>
- Otto A, Otto FEL, Boucher O, Church J, Hegerl G, Forster PM, Gillett NP, Gregory J, Johnson GC, Knotty R, Lewis N, Lohmann U, Marotzke J, Myhre G, Shindell D, Stevens B, Allen MR, 2013: *Energy budget constraints on climate response*. Nat Geosci, 6(6), 415–416. <https://doi.org/10.1038/ngeo1836>
- Quay P, Sonnerup R, Westby T, Stutsman J, McNichol A, 2003: *Changes in the $^{13}\text{C}/^{12}\text{C}$ of dissolved inorganic carbon in the ocean as a tracer of anthropogenic CO_2 uptake*. Glob Biogeochem 17(1), 4-1-4-20. <https://doi.org/10.1029/2001GB001817>
- Patterson RT, Prokoph A, Changa A, 2004: *Late Holocene sedimentary response to solar and cosmic ray activity influenced climate variability in the NE Pacific*. Sediment Geol, 172 , 67 – 84. <https://doi.org/10.1016/j.sedgeo.2004.07.007>
- Peristykh AN, Damon PE, 2003: *Persistence of the Gleissberg 88-year solar cycle over the last ~12,000 years: Evidence from cosmogenic isotopes*. J Geophys Res: Space Phys, 108 (A1), 1003. <https://doi.org/10.1029/2002JA009390>
- Ramanathan V, Cicerone R, Singh H, Kiehl I, 1985: *Trace gas trends and their potential role in climate change*. J Geophys Res 90, 5547-5566. <https://doi.org/10.1029/JD090iD03p05547>
- Revelle R, Suess HE, 1957: *Carbon dioxide exchange between atmosphere and ocean and the question of an increase of atmospheric CO_2 during the past decades*. Tellus, 9(1), 18–27. <https://doi.org/10.1111/j.2153-3490.1957.tb01849.x>
- Sabine CL, Feely RA, Gruber, Key RM, Lee K, Bullister JL, Wanninkhof R, Wong CS, Wallace DW, Tilbrook B, Millero FJ, Peng TH, Kozyr A, Ono T and Rios AF, 2004: *The oceanic sink for the anthropogenic CO_2* . Science 305, 367–371. DOI: [10.1126/science.1097403](https://doi.org/10.1126/science.1097403)
- Santer BD, Fyfe JC, Pallotta G, Flato GM, Meehl GA, England MH, Hawkins E, Mann ME, Painter JF, Bonfils C, Cvijanovic I, Mears C, Wentz GJ, Po-Chedley S, Fu Q and Zou C-Z, 2017: *Causes of differences in model and satellite tropospheric warming rates*. Nat Geosci 10, 478-485. <https://doi.org/10.1038/ngeo2973>
- Scafetta N, 2010: *Empirical evidence for a celestial origin of the climate oscillations and its implications*. J Atmos Sol-Terr Phy 72, 951-970. <https://doi.org/10.1016/j.jastp.2010.04.015>
- Schlesinger ME, 1986: *Equilibrium and transient climatic warming induced by increased atmospheric CO_2* . Clim Dyn, 1(1), 35–51. <https://doi.org/10.1007/BF01277045>
- Schlesinger ME, Ramankutty N, 1994: *An oscillation in the global climate system of period 65-70 years*. Nature, 367, 723-726. <https://doi.org/10.1038/367723a0>
- Schildknecht D, 2020: *Saturation of the infrared absorption by carbon dioxide in the atmosphere*. Int J Modern Phys B. <https://arxiv.org/pdf/2004.00708.pdf>

Schmidt GA, Ruedy R, Miller RL, Lacis AA, 2010: *Attribution of the present-day total greenhouse effect*. *J Geophys. Res.* 115, D20106. <https://agupubs.onlinelibrary.wiley.com/doi/full/10.1029/2010JD014287>

Schwabe SH, 1843: *Sonnenbeobachtungen im Jahre 1843 (in German)*. Observations of the Sun in the year 1843. *Astronomische Nachrichten* 21, 233–236. [10.1002/asna.18440211505](https://doi.org/10.1002/asna.18440211505)

Segalstad TV, 1998: *Carbon cycle modelling and the residence time of natural and anthropogenic atmospheric CO₂: On the construction of “greenhouse effect global warming” dogma. The continuing debate*. European Science and Environmental Forum (ESEF), Cambridge, England. 184–219. <https://www.researchgate.net/publication/237706208.pdf>

Shapiro AI, Schmutz W, Rozanov E; Schoell M, Haberleiter M. Shapiro AV, Nyeki S, 2011: *A new approach to the long-term reconstruction of the solar irradiance leads to large historical solar forcing*, *A&A*, 529, A67, 1-8. <https://doi.org/10.1051/0004-6361/201016173>

Smith CJ, Kramer RJ, Myhre G et al., 2018: *Understanding rapid adjustments to diverse forcing agents*. *Geophys Res Lett*, 45, 2023–2031. <https://doi.org/10.1029/2018GL079826>

Steinhilber F, Abreu JA, Beer J, Brunner I, Christl M, Fischer H, Heikkilä U, Kubik PW, Mann M, McCracken KG, Miller H, Miyahara H, Oerter H, Wilhelms F, 2012: *9,400 years of cosmic radiation and solar activity from ice cores and tree rings*. *PNAS*, 109(16), 5967–5971. <https://www.pnas.org/doi/10.1073/pnas.1118965109>

Stine AR, Huybers P, Fung IY, 2009: *Changes in the phase of annual cycle of surface temperature*. *Nature*, 457, 435–441. <https://doi.org/10.1038/nature07675>

Srivastava A, Verkouteren M, 2018: *Metrology for stable isotope reference materials: ¹³C/¹²C and ¹⁸O/¹⁶O isotope ratio value assignment of pure carbon dioxide gas samples on the Vienna PeeDee Belemnite-CO₂ scale using dual-inlet mass spectrometry*. *Anal Bioanal Chem* 410, 4153–4163. <https://doi.org/10.1007/s00216-018-1064-0>

Suess HE, 1980: *The radiocarbon record in tree rings of the last 8000 years*. *Radiocarbon*, 22(2), 200– 209. <https://www.cambridge.org/core/journals/radiocarbon/article/radiocarbon-record-in-tree-rings-of-the-last-8000-years/EBD9056098B2151DA8027942C338F514>

Trenberth KE, Fasullo JT, 2013: *An apparent hiatus in global warming?* *Earth’s Future*, 1, 19–32. <https://doi.org/10.1002/2013EF000165>

UAH, 2022: *UAH MSU temperature data set of lower troposphere*, http://vor-tex.nsstc.uah.edu/data/msu/v6.0beta/tlt/uahncdc_lt_6.0beta5.txt

Utrecht Universiteit, 2016: *Radiocarbon dating*, <http://web.science.uu.nl/AMS/radiocarbon.htm>

- Vedeler M, Jørgensen LB, 2013: *Out of the Norwegian glaciers: Lendbreen – a tunic from the early first millennium AD*. *Antiquity* 87, 788–801. <https://doi.org/10.1017/S0003598X00049462>
- Velasco Herrera VM, Mendoza B, Velasco Herrera G, 2015: *Reconstruction and prediction of the total solar irradiance: From the Medieval Warm Period to the 21st century*. *New Astron*, 34(), 221–233. <https://sci-hub.wf/10.1016/j.newast.2014.07.009>
- Vinther BM, Jones PD, Briffa KR, Clausen HB, Andersen KK, Dahl-Jensen D, Johnsen SJ, 2010: *Climatic signals in multiple highly resolved stable isotope records from Greenland*. *Quat Sci Rev*, 29(3-4), 522–538. <https://doi.org/10.1016/j.quascirev.2009.11.002>
- Vinther BM, 2011: *The medieval climate anomaly in Greenland ice core data*. *PAGES news*, 19(1), 27. [Vinther_2011-1_27.pdf](#)
- Wijngaarden W and Happer W, 2020: *Dependence of Earth's thermal radiation on five most abundant greenhouse gases*. <https://arxiv.org/abs/2006.03098>
- Wild M, Hakuba MZ, Folini D, Dörig-Ott P, Schär C, Kato S, Long CN, 2019: *The cloud-free global energy balance and inferred cloud radiative effects: an assessment based on direct observations and climate models*. *Clim Dyn* 52, 4787–4812. <https://doi.org/10.1007/s00382-018-4413-y>
- Zhang Y, Rossow WB, Lacis AA, Oinas V, Mishchenko MI, 2004: *Calculation of radiative fluxes from the surface to top of atmosphere based on ISCCP and other global data sets: Refinements of the radiative transfer model and the input data*. *J Geophys Res*, 109(D19), D19105–<https://doi.org/10.1029/2003JD004457>